This is the author's manuscript of the contribution published as:
Elisa Arduca, Michele Perego, Doping of silicon nanocrystals, Materials Science in Semiconductor Processing, Volume 62, 2017, Pages 156-170, ISSN 1369-8001, https://doi.org/10.1016/j.mssp.2016.10.054

Doping of Silicon Nanocrystals

Elisa Arduca and Michele Perego

Laboratorio MDM, IMM-CNR, Via Olivetti 2, Agrate Brianza Italy

Abstract

Over the last decades silicon nanocrystals (Si NCs) were the subject of an intense research activity, due to their optical and electronic proprieties. Different experimental approaches were developed to synthesize Si NCs embedded in a dielectric matrix as well as freestanding Si NCs with well controlled structural and morphological characteristics. Actually, as in the case of bulk semiconductors, the fine tuning of their optical and electronic properties is related to the effective capability to control doping, i.e. impurity incorporation within these nanostructures. Even if Si NCs doped with both p-type and n-type dopants were successfully synthetized, several fundamental issues need to be understood. First of all, from a structural point of view, it results very hard to obtain information about dopant location with respect to Si NCs surface and core. This uncertainty is related either to the intrinsic limitations of the experimental approaches for the synthesis and for the analysis of doped Si NCs, as to the difficulties in modeling these nanostructured systems. Moreover, from a fundamental point of view, it is not clear if impurity incorporation in Si NCs effectively results in the generation of free charge carriers as in the case of bulk silicon. This review presents an overview of the recent progress in the field, focusing on the latest results related to doping of Si NCs. In particular the problem of thermodynamic stability of impurities into Si NCs and the problem of modulation of electrical properties of Si NCs will be systematically addressed.

1. Introduction

Semiconducting nanostructures with reduced dimensionality have attracted considerable scientific interest due to their peculiar properties, arising from the interplay between quantum confinement and surface related effects. In fact, if at least one of the dimensions of nanostructures is smaller than twice the Bohr radius of the exciton in the bulk material quantum confinement occurs causing a different electronic and optical behavior in the nanostructures compared to bulk materials. Moreover, the reduced size of these structures causes a remarkable increase of the surface area to volume ratio (S/V). Consequently surface related defects may significantly alter the electronic behavior of the nanostructures [1]. Si nanostructures appears to be particularly appealing for application in several fields like microelectronics, optoelectronics, photovoltaics, plasmonics and thermoelectric [2]–[5]. During the last century, impurity doping of Si was used to tailor the electronic properties of bulk silicon, employing p/n junctions as common building blocks of Si-based electronic devices [6]. The exploitation of Si nanostructures as basic elements for the fabrication of complex optoelectronic and microelectronic devices requires the capability to effectively control their electronic proprieties by means of doping as in the case of bulk semiconductors.

In the last decades Silicon nanocrystals (Si NCs), i.e. ~~a~~ Silicon particles having diameter (d) smaller than 100nm and composed of atoms in either a single- or poly-crystalline arrangement, were the subject of an intense research activity, owing to their optical and electronic properties [7][8][9]. In Fig. 1(a) HRTEM images of a small Si-NC with spherical and nonocrystalline morphology is reported [10]. Furthermore, Si NCs represent a paradigmatic system because the attainable results are in the extreme case of nanoscaling, from bulk to 0D system, and therefore they are useful for the understanding of other systems with reduced dimensionality like nanowires, fins or nanosheet [11][12][13][14]. Several studies are available in the literature on the synthesis of Si NCs embedded in dielectric matrix and freestanding Si NCs [15]. Si NCs embedded in dielectric matrix have been synthesized by ion implantation [16][17][18], chemical vapor deposition (CVD) [19][20][21], e-beam deposition [22][23], sputtering [24]–[26] and reactive ion etching [27]. As an example, in Fig. 1(b) 3D atom map of Si NCs layer inside SiO_2 matrix obtained by Atom Probe Tomography (APT) is reported [28]. Most of these approaches are based on processes that are already employed in microelectronic industries to facilitate the integration of these nanostructures in functional microelectronic devices [29][30][31][32]. Conversely freestanding Si NCs have been synthesized by crumbling porous Si [33][34] or by

gas-phase approaches, which usually concern the decomposition of a Si precursor by means of thermal heating [35], laser ablation [36] or plasma [37][38][39]. Freestanding Si NCs open the route to the control of surface chemistry and are extremely interesting for the development of thermoelectric devices [40][41], single electron transport device [42][43], solar cell [44], cold electron emitting device [45] and optical device [46].

In the case of very small Si NCs quantum confinement phenomena play a important role in the definition of their electrical and optical properties. Since Bhor radius of an exciton in silicon is about 5 nm, quantum confinement has been widely reported for Si NCs with diameter smaller than 10 nm [17][48][49][50][51]. The most striking effect is related to the progressive increase of the band gap [15][16][18][26][37]. An example is shown in Fig. 1(c) [18] in which the band gap is increased from 1.2 eV (band gap of silicon bulk) up to 1.6 eV when decreasing the size of the nanostructures. On the other hand, surface related defects may appear as localized states within the band gap of Si NCs modifying even more the electronic behavior of Si NCs with respect to bulk silicon. Recent works investigated the band alignment of Si NCs embedded in a SiO_2 matrix as a function of the diameter, identifying three different regimes; primarily quantum confinement affects the conduction band that is shifted towards high energy values, then surface effects pin the conduction states, and finally quantum confinement modifies the valence band with a shift towards low energy values [1].

In systems confined as Si NCs many others important questions arise, as to whether the dopants could play a role similar to that in bulk silicon, where the presence of impurities alter the conductivity of the material by several orders of magnitude. Actually very small Si NCs have been successfully doped with both p-type (B) and n-type (P, As) impurities by means of different experimental approaches [53][54][55]. However there are some important issues that still need to be clarified. First of all very few data are available about the thermodynamic stability of impurity atoms in Si NCs [56]. This uncertainty is related to the intrinsic limitations of the experimental approaches for the synthesis and for the analysis of doped Si NCs, as well as to difficulties in modeling this nanostructured system [56]. Moreover the effect of impurities on the electronic properties of Si NCs is far from been understood. For instance it is not clear yet if the incorporation of impurities in Si NCs corresponds to the generation of free charge carriers [57][58].

The present review provides an overview of the most recent results related to doping of Si NCs. The manuscript is organized in two main sections: the first section focuses on the problem of

intentional introduction of impurities into Si NCs comparing the different theoretical and experimental results available in the literature. This section represents the main part of the present review. The second section of the manuscript faces the problem of the modulation of electrical properties in doped Si NCs, trying to correlate the experimental data on dopant incorporation with effective electronic characteristic of the silicon nanostructures.

2. Impurity incorporation into Si NCs

Among all the possible dopants of silicon, P and B represent by far the most common choice for n-type and p-type doping respectively. This is related to their good ionization efficiency at room temperature, since substitutional P and B atoms inside crystalline silicon introduce very shallow energy levels in the band gap resulting in the presence of free charge carriers in the conduction and valence bands of the semiconductor [6]. Indeed it is well known that, in bulk Si, P and B atoms are stably incorporated substituting Si atoms in the crystalline network [6]. Actually in the case of Si NCs the description of the system is much more complex. First of all it is necessary to take into account the enormous surface area of Si NCs. The NC surface may act as a trap for the impurity incorporation so that impurities may reside at the surface and not in the Si NCs core. Moreover, it is important to note that notion like “surface” and “core” are really tricky to define for very small structures.

According to several theoretical predictions, a change in dopant positioning within Si NCs should significantly affects the electrical activity of dopant atoms [59][60][61][62][63][64]. Experimentally it turns out that optical properties of Si NCs are severely affected by dopant incorporation within the Si NCs [54][60][65][66]. The optical activity of B and P impurities may also be closely related to dopant location. Actually it is hard to experimentally determine the dopant location inside Si NC with high precision. For this reason theoretical efforts have focused on detailed modelling of dopant location inside NCs [64][59]. Further difficulty in the understanding of dopant incorporation at the nanoscale is related to the fact that theoretical calculations usually refer to thermodynamic equilibrium conditions, whereas, in most of the experimental works, impurity incorporation is commonly performed during Si NC formation. [67][65][55][68][69][70][71] This latter circumstance makes difficult to experimentally decouple thermodynamic equilibrium properties from kinetic effects. For this reason the comparison between theoretical and experimental results is not straightforward. Moreover theoretical investigations are often performed on Si NCs with diameter well below the values that are

commonly attainable with standard synthesis techniques [14][72][73]. Over the years the mismatch has been reduced by progressively increasing the size of the Si NCs in the numerical simulations [74][75][63][76]. Finally it is important to highlight that Si NC surface plays an important role in determining kinetics and thermal stability of the incorporated impurities [14][59][74][77]. Consequently in the comparison among theoretical and experimental results, it is important to distinguish between freestanding Si NCs and Si NCs embedded in a dielectric matrix. This section provides an overall picture of the main theoretical and experimental results on the incorporation of dopants in small Si NCs trying to discriminate the different effects related to incorporation of dopant as a function of the size of the Si NCs and of their surface characteristics.

2.1 Theoretical Description

In the case of free-standing Si NCs with H-terminated surfaces, theoretical studies demonstrated that both B and P atoms thermodynamically prefer to reside at the surface of the silicon nanostructures in order to reduce the stress nearby the dopant atom and to saturate Si dangling bonds.[74] [63] [62] [78] Consequently, for this specific system, the doping of the nanocrystal core region is expected to be very difficult[73][79][80][72][48]. In particular Pi *et al.* studied the formation energies of substitutional P and B impurity atoms in doped H-terminated Si NCs with diameter d = 2.2 nm.[63] A variety of bonding configurations of B impurity atoms both inside Si NCs and at the NCs surface were investigated. Figure 2(a) reports the formation energy of substitutional B atoms as a function of the distance from the center of the Si NC. The thermodynamic stability of the doped Si NCs progressively increases when B moves from the Si NC center to the NC surface [63]. Interestingly in most of the considered configurations a B atom at NCs surface is three-coordinated. As a consequence B atoms trapped at the Si NC surface do not act as acceptors, in agreement with results reported by Polissky *et al.* in the case of Si NCs inside a porous Si matrix [81]. Similarly P impurity atoms are found to be most likely incorporated at the Si NC surface, as shown in Fig. 2(b) [62]. All the bonding configurations at NC surface correspond to three-coordinated P atoms, that are electrically inactive [62][78]. Nevertheless, the incorporation of P impurity atoms effectively disables the formation of dangling bonds at the surface, suppressing defect-induced non-radiative events [80]. This effect was not observed in the case of B impurity atoms.

For this specific couple of dopants, the relationship between H-terminated Si NCs size and formation energy of substitutional P and B impurities has been investigated in details. Theoretical predictions indicate that: smaller the Si NCs, larger the energy is needed for the formation of substitutional P and B atoms [73]. On the basis of these results, a sort of self-purification mechanism was proposed for very small Si NCs [82][83][84][85][86]. The basic idea is that, as dopant could induce stress inside crystalline core of Si NCs, expelling impurities toward surface could results in reduction of the energy of the system. In fact, stress induced by dopant can be accommodated by modification of surface geometry. Chan *et al.* using a real-space first-principles pseudopotential method investigated impurity incorporation in H-terminated Si NCs with diameter up to 6 nm. They found a critical Si NCs size (~2nm) below which the dopant atom is expected to be ejected to the surface [86]. Details of the self-purification have been a matter of discussion for long time [87], and a clear understanding of the relative role of kinetics and energetics is still incomplete. The possibility of using intrinsic defects to alter the self-purification mechanism and possibly stabilize extrinsic dopant atoms incorporated within small Si NCs has been studied as well. For very small B-doped Si NCs composed of 145 Si atoms, it was demonstrated that, if a vacancy can be introduced at the center of Si NCs, a B atom would preferentially stay in close proximity to the vacancy and become more stable in the Si NCs core [72].

For B and P co-doping of Si NCs with H-terminated surfaces, a clear theoretically prediction of dopants location is not available. Apparently dopant atom location depends on the doping level, i.e. on the ratio between number of dopant atoms and number of Si atoms within the Si NC. Ma *et al.* report that the incorporation of B and P inside the NC core only occurs during heavily doping, since B and P atoms are most likely located at the NC surface. They demonstrated that, in the case of light co-doping of a 2.2 nm diameter Si NC, B and P might be all located at the NC surface where there exist enough space for the steric relaxation of dopants. Furthermore the formation energy of light co-doped Si NCs is found to be between those of B and P doped Si NCs, and it is hardly affected by the distance between dopants [61]. Ossicini *et al.* reported that, in case of very heavy co-doping, B and P atoms tend to occupy the nearest neighboring sites in the subsurface layer of the Si NCs. Moreover they found that co-doping is always energetically favored with respect to B and P single-doping [88][75].

It is worth to note that free-standing Si NCs with hydrogen or halogen terminated surfaces have been experimentally synthetized. However they quickly oxidize when exposed to air even at

room temperature [89][90]. Moreover Si NCs embedded in a dielectric matrix have been widely investigated for their interesting electronic and optical properties. Their surfaces are characterized by peculiar bonding configurations with the elements of the surrounding matrix. Obviously, the chemical composition of the Si NC surface significantly affects the dopant-surface interaction and therefore it is important to theoretically understand how oxidation influences the energy of impurities formation. Comparison between fully H-passivated Si NCs ($Si_{147}H_{100}$) and partially H passivated one ($Si_{147}H_{99}$) suggested a different energetics of the imputity atoms in the Si NCs depending on their surface passivation. In particular for the latter case it was demonstrated that P atoms preferentially locate at surface sites while B atoms may reside in the core of the Si NCs [76]. From a general point of view, for substitutional group III and group V elements, it is shown that the presence of a surface oxygen layer drastically changes the radial dependence of the dopant formation energy. In the Si NCs with silanol surface groups (Si-OH), the formation energy of dopant impurities displays variation of few electron volts, featuring, for most dopant species, a lower energy in the region below the surface and a higher energy at surface sites [59]. In the case of P-doped small Si NCs (87 atoms), it has been demonstrated that the presence of silanol surface groups cause a segregation to an outer shell close to the surface, where P is not directly linked to H or OH. Moreover, it suppress the formation of tri-coordinated surface defects [78]. In the case of B and P co-doping of small Si NCs (87 Si atoms) with silanol surface groups, it is revealed that the formation of a P-B bond is energetically favoured, with B positioned at the NCs surface and P at the inner nearby[14]. Ni *et al.* [91] studied P doping of a Si NC (d = 1.4 nm) covered by a 0.25 nm thick SiO_2 layer. P atoms resulted the most likely incorporated into the sub-interface of Si/SiO_2 interface. Moreover, according to their simulations, for Si NCs with dangling bonds at the Si/SiO_2 interface, a P atom prefers to passivate the dangling bond. These theoretical results suggest that the presence of dangling bonds and SiO_2 shell at the Si NCs surface helps reducing the binding energy of P in Si NCs.

In particular the case of P^+ doped 1.5 nm Si NCs covered by a 2 nm-thick amorphous SiO_2 shell was studied in terms of energy formation of impurity atoms within the Si NCs. Fig. 2 (f) shows a pictorial view of an undoped Si NC obtained from molecular dynamics simulations [74]. Unlike H- or OH-terminated Si NCs, in SiO_2 covered Si NCs P^+ ions are found to be more stable in the Si NCs core than at the surface, as shown in Fig. 2 (d) [74]. In fact, in the SiO_2 covered Si NCs the lattice defects at the interface between the Si core and the SiO_2 shell help to release the strain

in the Si core and, therefore, chemical bonding effect predominates. The preference of P for the Si core is thus driven by the lower energy necessary to form a P^+-Si bond at the expense of a Si – Si bond, as compared to the energy necessary to form a P^+-O bond at the expense of a Si-O bond. In the case of B-doped 1.5 nm diameter Si NCs surrounded by an outer shell of SiO_2 with a thickness of about 0.5 nm, the calculated formation energy suggest that B is equally stable in the Si core and in the SiO_2 shell, showing preference for interface sites, as depicted in Fig. 2 (c) [77]. Actually the cost of replacing Si-Si bonds by a B-Si bond is approximately the same as the cost of replacing a Si-O bond. Moreover, it is shown that the energy formation is closely related to the bond lenght: the shorter B-Si bonds, the more stable the structure. Since closer to the interface B-Si bonds are on average shorter than in the bulk, this may explain why interface sites are favorite.

Recently theoretical works addressed the subject of doped Si NCs embedded in a solid matrix [14][92]. In the case of very small Si NCs that are composed by 35 atoms, the data indicated that for n-type doping (P and N) the impurity atoms tend to settle the NC core, while for p-type doping (Al and B) the interfacial sites are favored. The energetics of the system as a function of the dopant position shows that SiO_2 forms a very large diffusion barrier for P and N, and a much reduced one for B and Al. Total energy for impurity formation is reported in Fig. 2 (e) [14][92]. According to these data, the preferential location of the impurity seems to be strongly correlated with the electronegativity [14].

2.2 Experimental Results

Several works reported doping of Si NCs with B and P, for free-standing Si NCs as well as for Si NCs embedded in a solid matrix. Several experimental approaches have been implemented to achieve this goal. Clear information about the effective positioning of dopant atoms within the Si NCs are difficult to obtain and data available in the literature on this specific topic are scarce and conflicting. This section provides an overall picture of the main experimental results about dopant incorporation in Si NCs. Literature data are critically reviewed focusing on the problem of thermodynamic stability of dopant atoms. The section is organized in two parts that provide information about the doping of freestanding and embedded Si NCs respectively.

2.2.1 Freestanding Si NCs

Many different techniques have been implemented for the synthesis of free-standing Si NC like, for instance, solid-gas reaction, thermal decomposition of silane, laser pyrolysis of silane, laser ablation of solid silicon targets, non thermal plasma synthesis or solution route [15]. In particular the plasma based methods have been proved to be very efficient in producing high quality Si NCs with limited defectivity and a very high control over their size distribution [93]. To date, the plasma-based methods have also been demonstrated to be extremely efficient in the synthesis of doped Si NCs. Interestingly in recent papers, Ni *et al.* have reviewed the literature related to the synthesis of doped Si NCs by plasma routes [94], while Pereira published an interesting review about the doping of semiconductor nanoparticles synthetized in gas-phase plasmas [93].

Actually free-standing B and P doped Si NCs are readily produced by adding B and P precursor during the plasma process for the synthesis of intrinsic Si NCs [37][39][95]. In this case impurity incorporation is performed during NC formation. The most widely used dopant precursors are diborane (B_2H_6) and phosphine (PH_3) [80][96][97][98][99]. Recently it has been shown that also organic dopant precursors, like TMP or $P(OCH_3)_3$, could be efficiently employed for the doping of Si NCs, providing a safe and economical solution to the problem [100]. Varying the ratio of silane to dopant precursor, it is possible to effectively control dopant concentration within the Si NCs over a fairly wide range of values [97][80]. In these systems, dopant levels ranging from 10^{18} up to 10^{22} cm^{-3}, that corresponds to a maximum of 1 at.%, are usually reported both for P [101][80][102] and B [102][41][103]. Moreover very high concentrations are possible leading to the so called hyperdoped free-standing Si NCs with dopant concentration of 20 at.% for P and 30 at.% for B [96]. It is worth to note that these dopant concentrations correspond to average values, without any distinction between dopant atoms trapped at the Si NC surface and incorporated in the Si NC core.

In order to understand dopant location, several experimental approaches have been implemented using different techniques that provide information about the local environment of the incorporated dopant atoms. Pereira *et al*. used electron paramagnetic resonance (EPR) to demonstrate the presence of P in substitutional location for P-doped Si NCs (4 nm < d < 50 nm) grown in a low pressure, flow-through microwave plasma reactor [104][101]. Using electrically detected magnetic resonance (EDMR), the presence of P atoms in substitutional location was observed also in P-doped Si NCs (5 nm < d < 10 nm) produced using a very high frequency plasma deposition system[105]. The combination of X-ray Photoelectron spectroscopy (XPS)

and EPR data indicated that P atoms can be introduced into substitutional sites within Si NCs grown in a high frequency non-thermal plasma system using organic dopant precursor [100]. Pi *et al.* compared the concentration of B and P in ~3.6 nm Si NCs before and after removal of surface oxide by HF treatment [60]. Effective reduction of dopant concentration in Si NCs upon HF etching is shown in Fig. 3 (a). Experimental data suggest that B atoms are preferentially located in the Si NC core, while P atoms reside at the NCs surface. The different distribution of B and P atoms in plasma-synthetized Si NCs was detected also by Stegner *et al.* [80] and Zhou *et al.* [96] in similar but independent experiments. In particular Stegner *et al.* measured P concentration in Si NCs before and after etching of the SiO_2 outer shell by secondary ion mass spectrometry (SIMS). Experimental data are reported in Fig. 3 (b). Interestingly Pi *et al.* reported a percentage of P in the thin SiO_2 outer shell of Si NCs, that is ~80%. This value is significantly lower than the one (~95%) observed by Stegner *et al.*. The reason for this difference is unclear. Perhaps it could be related to the higher temperature experienced by the P doped Si NCs during growth in microwave plasma reactors when compared to RF plasma reactors. This could enhance the diffusion of P atoms towards the surface. The difference could also originate from a longer plasma residence time in the case of Si NCs grown in microwave reactors [93]. Rowe *et al.* observed a similar P distribution within heavily doped ~10 nm Si NCs synthetized in a RF capacitively coupled non-thermal plasma system. Scanning transmission electron microscopy (STEM) imaging with energy-dispersive X-ray spectroscopy (EDX) measurements suggested that P is either incorporated into the Si NCs and/or condensed at the Si NC surfaces. The presence of surface $Si{-}P_x{-}H_y$ vibrations in localized surface plasmon resonance (LSPR) analysis indicated the occurrence of a significant P segregation at the surface. P concentration inside Si NCs has been measured before and after wet chemical etching of native oxide shell surrounding Si NCs, results suggest that 60−75% of P is condensed on the NC surface, as shown in Fig. 3 (c) [106].

As discussed in the previous section, theoretical simulations predicted that, in the case of Si NCs covered by an amorphous SiO_2 shell, P atoms are more stably incorporated in the Si NC core [74], while B atoms appear to be equally stable in the Si core and in the SiO_2 shell, showing a clear preference for interface sites [77]. It is clear that the theoretical picture based on the assumption of thermal equilibrium may not apply for doping of Si NCs during their synthesis in plasma. Impurity incorporation during NC formation makes hard to experimentally decouple equilibrium properties from kinetic effects. In their study on hyperdoped Si NCs, Zou *et al.* [96]

suggested that doping in non-thermal plasma systems is mainly controlled by kinetics. They designed a simplified kinetics model in which the resulting dopant concentration is basically determined by the frequency of collision between impurities and Si NC. The collision may lead to the adsorption of B and P atoms on the Si NCs surface and the adsorbed B or P atoms could then be trapped during the subsequent growth of Si NCs. Collision frequency is shown to strongly depend on impurity mass, so it is clear that collision frequency for B is larger than that for P. Consequently B atom concentration can reach 30 at.% while P is limited to 20 at.%. This model is designed in order to explain why Si NCs can be doped with B or P to concentration that are well beyond the solubility limit (1 at.% for B and 0.3 at,% for P [107]) of these impurities within bulk silicon. Interstingly very high dopant concentrations were observed also in freestanding Si Ncs obtained using solution synthetic methods. In solution routes, suitable precursors are reacted in an inert atmosphere to reduce the possibility of oxidation [51]. Reduction of a mixture of $SiCl_4$ and PCl_3 with Mg results in P-doping at about 6% atomic concentration in Si NCs (5-12 nm), that is much higher than solubility limit in bulk silicon [108]. In conclusion, experimental results on doped freestanding Si NCs undoubtedly demonstrate that B and P impurity incorporation into Si NCs is kinetically possible. Unfortunately, for freestanding Si NCs, data available in the literature have been obtained following doping strategies that do not allow decoupling impurity incorporation from Si NC formation. Consequently these experimental results do not give information about thermodynamic stability of dopants inside Si NCs.

2.2.2 Embedded Si NCs

Actually Si NCs can be easily synthesized within a dielectric matrix using a two-step process involving the formation of a silicon supersaturated film, followed by annealing at high temperature in an inert atmosphere. During the thermal treatment, the silicon supersaturated film, which can be an oxide, nitride or carbide, undergoes a phase separation, resulting in the nucleation of Si NCs embedded in an amorphous dielectric matrix [15][8]. Several approaches have been proposed to form these silicon supersaturated films within a SiO_2 matrix, including sputtering [69][109][110], plasma-enhanced chemical vapor deposition [111], ion implantation [70][112] and reactive ion etching [113]. In this case doping of Si NCs has been usually performed by introducing dopant impurities in the matrix before NCs formation and subsequently inducing dopant incorporation and Si NCs formation simultaneously. Although

widely employed in the literature, this approach makes basically impossible to experimentally decouple equilibrium properties of the system from kinetic effects. For this reason, more recently, significant efforts have been performed to develop alternative approaches that allow doping Si NCs after their formation. Consequently this section has been organized in two parts. In the first part, we systematically review the results about successful doping of Si NCs that were achieved by experimental approaches in which doping and synthesis occur together. In the second part, we focus on the experimental results that were achieved by decoupling synthesis and doping steps.

Doping during Synthesis

In 1996 Fujii *et al.* reported for the first time on the effective doping of B atoms into Si NCs dispersed in a ~2μm thick borosilicate glass. Samples were prepared by cosputtering of Si, SiO_2 and B_2O_3 targets and subsequent annealing at high temperature [69]. The growth of Si NCs in the matrix was demonstrated by high-resolution transmission electron microscopy (HRTEM), while the doping of B atoms into Si nanocrystals was been confirmed by Raman spectroscopy. In this method, the size of NCs could be controlled varying the effective silicon concentration in the matrix, i.e. the number of Si targets during cosputtering, and/or by changing the annealing temperature. Similarly, overall B concentration in the oxide film is finely tuned by adjusting the number of B_2O_3 targets during cosputtering. The authors reported that the photoluminescence (PL) is drastically quenched with increasing B concentration, as shown in Fig. 4 (a). The decrease in the PL efficiency is explained assuming B atoms are incorporated within the Si NCs in substitutional sites. Indeed, substitutional B atoms introduce free carriers (holes) that led to non-radiative Auger recombination effect, which efficiently quench natural PL emission in Si NCs [114]. In a subsequent work on B doped Si NCs synthetized by this cosputtering method, Xie *et al.* suggested the concurrent presence of B atoms in substitutional sites within Si NCs and in the oxide film and/or interface between Si NCs and the surrounding matrix [115]. Fig.5 (a) show the high resolution XPS spectra of B 1s core level corresponding to a change of the total B concentration in the oxide films from 0.59 at.% to 5.43 at.%. The presence of a B-O component in the XPS spectra suggests the existence of B atoms in the SiO_2 matrix and/or at the Si NCs/SiO_2 interface. The B-B/B-Si component indicates that B atoms exist in substitutional sites inside Si NCs. Accroding to these data the amount of B atoms trapped into Si NCs ranges from 0.25 at.% for the sample with the lowest B concentration to 2.32 at.% for the sample with the

highest B concentration. No evidence of a self-purification phenomenon is observed irrespective of thevery small size ($2 < d < 15$ nm) of the Si NCs.

The same cosputtering method was used to synthesize P doped Si NCs dispersed in a phosposilicate glass [116]. Fig. 4 b) shows an initial increase of PL efficiency in lightly doped Si NCs [116][67], followed by a sudden decrease of PL emission when the P concentration further increases [117][118]. Fujii *et al.* explained the PL enhancement observed at low P concentration, as a consequence of the passivation of interface defects such as dangling bonds by P atom impurities [116]. At high P concentration P atoms introduce free carriers that, leading to Auger effect, induce a significant decrease of PL efficiency [67]. It is worth to note that PL measurements do not provide any direct measurement of effective dopant location inside NCs. Indeed, the assumption that PL efficiency variations are linked to different impurity position within the Si NCs is based on knowledge acquired on free carriers in bulk Si. Nevertheless this knowledge transfer from bulk to nanostructured silicon might be misleading because a delocalized carrier inside a NC remained physically confined by the NC [62].

Doped Si NCs embedded in a SiO_2 matrix can be synthesized by means of a superlattice approach [119][57]. It has been demonstrated that phase separation and thermal crystallization in SiO/SiO_2 superlattices result in the formation of 2 dimensional layers of Si NCs separated by thin SiO_2 layers [120][50]. P doping is commonly achieved by selectively adding a diluted phosphine gas (PH_3) during the superlattice deposition process. This technique permits to add dopants either to the Si rich layer or to the matrix separation layer or both. This allows a careful adjustment of the total dopant concentration. Recently Gutsch *et al.* demonstrated that for Si NCs with average size from 3nm to 4 nm, P concentration in Si NCs can be finely tuned from 1.15 at.% to 1.75 at.%. Moreover they observed that PL peak maximum exhibits a blueshift as doping concentration increase, while PL intensity progressively decreases. Moreover, a decrease of PL intensity is observed after hydrogen passivation. These trends are attributed to the preferential doping of larger Si NCS, which results in the effective removal of their PL contribution due to Auger recombination inducing PL quenching [119]. On a similar system, Gutsch *et al*. highlighted the low doping efficiency of substitutional P as compared to the large amount of P usually detected in Si NCs. They proposed that P atoms may not necessary occupy substitutional lattice sites but are rather incorporated as interstitial or P vacancy pairs [57]. Subsequently, based on experimental results about electronic transport in P doped Si NCs, Konig *et al.* suggested that

P atoms predominantly reside in interstitial sites [58]. More recently, Gnaser *et al.* prepared a multilayer structure with P doped Si NCs (2.9 nm < d < 4.5 nm) embedded in a SiO_2 matrix. 3D atom probe analysis (APT) the precise localization and the proper amount of P atoms inside the samples was accurately derived in a quantitative way. Fig. 5 b) shows the results of the APT. A significant P enrichment at the Si NCs/SiO_2 interface is detected (top) and P concentration inside Si NCs is observed to strongly decrease as Si NCs size decreases (bottom) [55]. The authors suggest that this trend could be considered as an experimental confirmation of the occurrence of a self-purification mechanism in very small Si NCs. Actually, the link between the preferential doping of large Si NCs and the self-purification mechanism is not trivial since doping of the Si NCs was achieved out of equilibrium during the Si NC synthesis. As a matter of fact, the preferential doping of larger NCs could be related to the probability of P atoms to be trapped in Si NCs if they can bind to their surface for a residence time comparable to the reciprocal growth rate, that is obviously higher for larger NCs.

Actually, efficient incorporation of P atoms in 2 nm Si NCs was demonstrated in a quite similar system, suggesting that preferential doping of large Si NCs reported by Gnaser *et al.* is strongly dependent on the specific experimental approach that is used for dopant introduction. In more details, Perego *et al.* prepared a SiO/SiO_2 superlattice structure by e-beam evaporation and introduced an ultrathin (thickness < 0.5 nm) P-SiO_2 layer close to the SiO film. [121][122] This approach allow to deliver a controlled amount of P atoms in the Si-rich region and to incorporate them in the Si nanocrystals during the subsequent high temperature thermal treatment. In order to obtain information on diffusion and segregation phenomena in Si NCs/SiO the samples were annealed at different temperatures (900° C and 1000° C). TEM images demonstrated that Si NCs average diameter is equal or smaller than 2nm. Time-of-flight secondary ion mass spectrometry (ToF-SIMS) results indicate a segregation of the P atoms in the Si NCs region during thermal treatment. The incorporation of P impurities within Si NCa is supported by XPS chemical analysis. Fig. 5 c) shows the high-resolution XPS spectra of the P 2*p* core level region in the as deposited and annealed samples. Data highlight an increase of the P-Si signal with increasing annealing temperature, indicating that the P atoms are definitely incorporated within the Si NCs. The opposite trend is observed for the signal related to P-O. P incorporation in Si NCs is explained considering that P diffusion in SiO_2 is much lower than in Si, and, consequently P diffusion towards the Si-rich region is strongly favored as revealed by ToF-SIMS analysis. Moreover, P atoms in an SiOx matrix have been shown to preferentially form P–Si or P–P bonds

[123]. Accordingly for P atoms it is energetically favorable to move in the Si-rich region forming P–Si bonding. It is well known that nanocluster nucleation and growth occurs during the very first stages of the thermal treatment. Long annealing times are usually required to crystallize the amorphous Si nanostructures. In this picture the P atoms are expected to segregate and to be trapped in the Si nanocluster region during the first stages of the thermal treatment. Although no information is available on P diffusivity in Si nanostructures we can assume that the probability for a P atom to leave the Si-rich region where Si nanocrystal formation occurs is limited by the low diffusivity of P in the SiO_2 surrounding matrix. This fact increases the probability for the P atom to be trapped in the Si nanocrystals under formation.

Interestingly, Khelifi *et al.* [70] demonstrated that co-implantation, with overlapping projected ranges of Si and P or As, in a 200 nm thick SiO_2 film followed by thermal annealing is an efficient way to form doped Si NCs (average size 2 nm) embedded in SiO_2. APT is used to image directly the spatial distribution of the various species at the atomic scale, evidencing that the P and As are efficiently introduced inside the Si nanocrystals. Their APT data do not show any evidence of P accumulation at Si NCs/SiO_2 interface, in contrast with data reported by Gnaser *et al*. [55].

In conclusion, these experimental results demonstrated that dopant incorporation into NCs is kinetically possible. However the presence of impurities during the Si NCs synthesis significantly affect the growth kinetics of Si NCs. This is corroborated by the observation of size variation of the resulting Si NCs as a function of the nature or concentration of dopant impurities, as shown in Fig. 5 d) [70][115]. Some authors claims to have experimentally demonstrated self-purification mechanism due to the observed preferential P doping of larger Si NCs (4.5 nm size) with respect to the smaller ones (2.9 nm size) [55]. Conversely other authors demonstrated that very small NCs (2nm size) can be effectively P doped during their growth [121]. As a matter of fact, the absence of thermodynamic equilibrium during the realization of these experiments does not allow to elucidate the mechanism of dopant incorporation within Ti NCs and to finally confirm the real occurrence of a self-purification phenomenon in very small Si NCs.

Doping after synthesis

An alternative strategy for the doping of Si NCs is to introduce dopant impurities after the synthesis of Si NCs. The most popular approach consists in the doping of Si NCs by means of

P^+ ion implantation. Many literature works focused on Si NCs embedded in thick SiO_2 (0.1 μm - 0.6μm). P ions were implanted with a dose ranging from 10^{13} cm^{-2} to 10^{17} cm^{-2}. Implantation was followed by thermal annealing at high temperature in order to reduce implantation defects and restore the original Si NC structure [124][125][126]. By XPS analysis, Kovalev *et al.* [124] observed that upon annealing P atoms redistributed between the SiO_2 matrix and Si NCs. Kachurin *et al.* [68] studied the effects of implantation of P ions on the PL of Si NCs as a function of the different doses (from 10^{13} cm^{-2} to 10^{16} cm^{-2}) and annealing temperatures at 600–1100 °C. Quenching of PL emission is observed immediately after ion implantation, due to the defects in Si NCs induced by ion implantation. The annealing temperature for the recovery of PL emission increases with P implanted doses. Moreover the PL intensity exhibits a clear dependence on the dose of implanted P ions, indicating that P atoms penetrate into Si nanocrystals. Similarly, Tchebotareva *et al.* [126] demonstrated that doping with P atoms at concentration up to 3 10^{19} cm^{-3} lead to a PL enhancement, followed by a progressive decrease in the PL intensity when further increasing P concentration. On the basis of previous data reported by Fujii et al. [116], PL enhancement is assumed to be associated with P surface passivation while the decrease in the PL intensity is attributed to Auger recombination due to presence of P inside Si NCs[117]. It is important to note that, in these experiments, even if the introduction of dopant in Si NCs is performed after the synthesis of the nanostructures, the implantation damage alters the initial equilibrium resulting in some cases in the complete amorphization of Si NCs. Consequently the incorporation of P atoms does not really occur at thermodynamic equilibrium since the dopant redistribution within the sample is accompanied by a Si NCs recrystallization.

An alternative experimental approach has been recently proposed in set of papers published by Perego *et al.* [127] and Mastromatteo *et al.* [128][129]. In their experiments the incorporation of P atoms in Si NCs was promoted after their formation, by delivering a controlled amount of dopant atoms from a spatially separated diffusion source. Si NCs embedded in thin SiO_2 film (about 20 nm) were prepared by e-beam evaporation of a SiO_2/SiO/SiO_2 multylayer structure and subsequent annealing at high temperature (1150°C, 60 min). After NCs formation, a thin (0.4 nm) layer of P-SiO_2 was evaporated on the top of SiO_2 film and *in-situ* capped with a 20 nm thick SiO_2 film. To promote P diffusion and trapping in Si NCs without perturbing the equilibrium structure of the Si NCs, thermal treatments were performed at temperature lower than the one used for Si NCs synthesis. TOF SIMS profiles of the samples before and after P diffusion are reported in Fig. 6 a). P profiles are overlapped to EFTEM images of the as-prepared

samples. EFTEM data about Si NCs size distribution and crystallinity before and after P diffusion demonstrate that Si NCs were not affected by the subsequent annealing processes at lower temperature. This means that the energetics of trapping/detrapping of P in the NCs are really measured at equilibrium, avoiding kinetic effect due to NC formation or evolution. The combination of TOF SIMS and XPS data demonstrated that, during the annealing process, the diffusing P atoms are efficiently trapped in the Si NC region and incorporated in the core of nanostructures or in a sub-interface region exhibiting no bonds with O. Actually the sensitivity of XPS measurement does not allow to excluding the presence of a residual amount of P atoms in surrounding SiO_2 matrix. Nevertheless the P concentration is at least 6 times the solubility in the bulk material, suggesting an increase of solubility in Si nanostructures. The experiment demonstrated that high levels of impurities can be introduced in the inner part of Si NCs in a stable configuration and the dopant content can be finely tuned by properly adjusting the annealing conditions.

These results represent the first evidence that P doping of Si NCs in SiO_2 corresponds to a thermodynamically favored configuration of the system. Quantitative physical information about the energetics of the system were extracted by fitting the calibrated ToF-SIMS profiles using a diffusion model based on Fick's law in one dimension [129]. From this analysis the capturing efficiency of the clusters, the P diffusivity rate in SiO_2 and the rate at which a single P atom escapes from the clusters were extracted. Fig. 6 b) shows Arrhenius plot of diffusion and release rates. As shown in the inset of Fig. 6 b), the acquired data allows depicting the energy scheme of the system highlighting that P atoms are thermodynamically favored to be trapped in the Si NCs with a binding energy of 0.9 eV. Since this energy was measured at equilibrium, the value can be safely compared with those obtained by ab-initio calculations. Indeed the binding energy value is in perfect agreement with the value of 1eV reported by Ni *et al.* for P doped 1.4 nm Si NCs surrounded by a 0.25 nm thick SiO_2 shell [91]. This experimental approach discloses opportunities for fundamental studies concerning the physics of doped Si NCs, providing a pathway to clarify the energetics of doping process. Similar experiments are necessaries to study B binding energy in Si NCs. Moreover a systematic study of the variation of dopants binding energy as a function of NCs size is still missing. These experiments could shed a new light on the rich physics of these nanostructures, investigating equilibrium phenomena predicted by theoretical works, like self-purification.

3. Electrical activity

Impurity doping of bulk Si has been widely used to tune the electronic properties of silicon by introducing free carriers that significantly modify its intrinsic conductivity. Doping of Si NCs is performed to achieve the same goal, i.e. control the electrical and optical responses of these nanostructures by the controlled introduction of free carriers. Actually, a clear understanding of the evolution of the effective carrier density in Si NCs as a function of impurity concentration is still lacking. In particular experimental data collected so far suggest that the capability of dopants to provide free carriers in Si NCs strictly depends on the synthesis method that was used to realize the nanostructures. In this section we briefly summarize the available experimental results about dopants activitation within small Si NCs. Theoretical studies on electron and hole transport induced by B or P substitutional doping in Si NCs embedded in a SiO_2 matrix were sistematically reviewed by Pi [64]. For further information about theoretical investigation about dopant activation in Si NCs we postpone interested reader to the recent work of Garcia-Catello *et al.* [92]. Once again the experimental results are reviewed considering the two cases of freestanding and embedded Si NCs respectively.

Freestanding Si NCs

Zhou *et al.* [96] studied B- and P-hyperdoped ≈14 nm Si NCs produced in a non-thermal plasma system. They demonstrated that both B and P atoms may be effective dopants for Si NCs. P-hyperdoping was found to induced significant enhancement of the oxidation of Si NCs, that implies that P atoms are effective donors. In fact, as the concentration of electrons in P-hyperdoped Si NCs is larger than that of undoped Si NCs, more electrons may tunnel through the oxide to reach the surface, ionizing more O atoms. The electrical activity of B was investigated by means of the Fano effect [130]. Si NCs B hyperdoped (7 at.% - 31 at%) were characterized by Raman spectroscopy. Fig. 7 a) shows Raman spectra obtained using two different excitation wavelengths. With the increase of the excitation wavelength the Raman peak at 517 cm^{-1} was broadened toward high wavenumbers. An anti-resonance dip also appeared on the low-wavenumber side of the 517 cm^{-1} peak. These features are both characteristic signatures of the Fano effect, indicating that there are B atoms that act as acceptors in these Si NCs. In a subsequent work on similar samples with hyperdoped Si NCs, Zhou *et al.* [131] found that when the doping levels of B and P are similar, the LSPR energy of B-doped Si NCs is higher than that of P-doped Si NCs because B atoms are more efficiently activated than P atoms in Si NCs.

In the case of P doped Si NCs synthetized in a plasma system, EPR data proved that donor electrons are present [104][132]. As depicted in Fig. 7 b), a clear resonance centered at g = 1.998 and two further lines denoted hf(^{3}1P) were observed. These features are a clearly fingerprint of substitutional, isolated P atoms trapped in the Si NC core [80]. In films formed by Si NCs doped with substitutional P atoms [101][104], it was observed that an increase of the NCs doping concentration resulted in an increase of the film conductivity and in a decrease of the temperature dependence of the conductivity. Using electrically detected magnetic resonance (EDMR) it was demonstrated that at low temperature both Si-dangling bonds of the surface and isolated substitutional P states participate in charge transport, showing that charge transport involves electronic states of NC cores and does not take place solely through surface states [101]. All these results proved that the donor electrons that are present in the Si NCs effectively contribute to charge transport enhancement in Si NCs. Nevertheless a complete picture about the effective impact of doping on charge transport in Si NC films is not yet available because effects like charge trapping in defect states, percolation of charges, and dopant ionization in NCs at room temperature may obscure the effect due to doping of the individual NCs. An example of influence on charge transport due to defect is reported by Lechner *et al.* [71]. They demonstrated that both P and B doping becomes effective dopants only when the concentration of dopant atoms overcomes the concentration of defect traps. Moreover, Pereira *et al.* [133] observed that, in films of Si NCs with a native oxide shell synthetized by plasma, no significant enhancement of conductivity is detectable even when P concentration is very high (5 10^{20} cm^{-3}). Thus, in surface-oxidized Si NCs, charge transport is not limited by the amount of available charges. This indicates that in films of surface-oxidized Si NPs inter-NP charge transfer involves the participation of oxide-related electronic states, whereas in H-terminated Si NP films direct inter-NP charge transfer plays a major role in the overall charge conduction. In recent reviews both Ni [94] and Pereira [93] summarize results about electronic properties of doped Si NCs synthetized by plasma providing an exhaustive description of the experimental results.

Embedded Si NCs

In the case of P doped Si NCs superlattices embedded in SiO_2 matrix synthetized by PECVD method, transient current analysis demonstrated that the effective concentration of electron available for current transport within the P doped NC conduction band corresponds to only 0.12% of the total P concentration [57]. This result is suggested to be a consequence of the

incorporation of P dopants in the NCs as interstitial impurities rather than as substitutional donors [57] [58]. In fact, on the basis of density functional theory calculations, interstitial P dopants in Si NCs are expected to introduce deep trap states which cannot donate electrons but provide efficient carrier recombination [58]. Nevertheless, doubling the P concentration yields twice the amount of carriers [57]. Fig. 7c) reports free carrier density derived from transient current analysis as a function of bias voltage. Analysis was performed on samples with different total P concentration. In a very recent work Almeida *et al.* [132], using EPR spectroscopy studied P doping of 5 nm Si NCs synthetized by cosputtering method. Fig. 7 d) shows the EPR spectra and the corresponding numerical fitting curve. Data indicate that most P dopants are incorporated at substitutional sites of the NCs lattice and thus effectively act as donor. Moreover they observed that the donor electron density decreases by several orders of magnitude when the NCs treated in HF to remove the native SiO_2 matrix and subsequently exposed to air. They interpreted this observation as charge compensation of P donors in the NCs by traps associated to molecules adsorbed to NC surface. Interestingly the process can be completely reverted by desorbing the molecule from Si NC surface under vacuum. The extreme difference in terms of dopant activation for the P doped Si NCs embedded in SiO_2 matrix synthetized by PECVD method and those synthetized by cosputtering method, suggests that, as the doping efficiency depends on dopants locations, the synthesis method can affect the donor electron distribution within the Si NCs. Unfortunately no experimental techniques are able to provide a direct measurement of the P distribution within the Si NCs. All the informations are usually obtained by indirect measurements and interpretation models whose validity has not been completely assessed yet.

4. Conclusions

In this work we provide an extensive review of the most recent experimental and theoretical results about doping of Si NCs. Introduction of dopant impurities in very small Si NCs have been achieved using several approaches. However the effective positioning and thermodynamic stability of the dopant impurities within the Si NCs are not clear and represent the subject of a intense research activity. Recent experimental results about Si NCs embedded in a dielectric matrix suggest that P impurities are incorporated within the core and/or in the region below the Si NCs/SiO_2 interface. The P atoms are demonstrated to be thermodynamically stable in agreement with theoretical prediction. Nevertheless the effective activation of these impurities

i.e. the availability of free charges in the Si NCs is questionable. Actually a complete theoretical and experimental description of the energetics of these systems is still missing.

References

[1] G. Seguini, C. Castro, S. Schamm-Chardon, G. Benassayag, P. Pellegrino, and M. Perego, "Scaling size of the interplay between quantum confinement and surface related effects in nanostructured silicon," *Appl. Phys. Lett.*, vol. 103, no. 2, 2013.

[2] M. C. Beard, K. P. Knutsen, P. Yu, J. M. Luther, Q. Song, W. K. Metzger, R. J. Ellingson, and A. J. Nozik, "Multiple exciton generation in colloidal silicon nanocrystals," *Nano Lett.*, vol. 7, no. 8, pp. 2506–2512, 2007.

[3] J. Tang, H. T. Wang, D. H. Lee, M. Fardy, Z. Huo, T. P. Russell, and P. Yang, "Holey silicon as an efficient thermoelectric material," *Nano Lett.*, vol. 10, no. 10, pp. 4279–4283, 2010.

[4] F. Priolo, T. Gregorkiewicz, M. Galli, and T. F. Krauss, "Silicon nanostructures for photonics and photovoltaics," *Nat. Nanotechnol.*, vol. 9, no. 1, pp. 19–32, 2014.

[5] R. Gresback, N. J. Kramer, Y. Ding, T. Chen, U. R. Kortshagen, and T. Nozaki, "Controlled doping of silicon nanocrystals investigated by solution-processed field effect transistors," *ACS Nano*, vol. 8, no. 6, pp. 5650–5656, 2014.

[6] Sze, *Physics of Semiconductor Devices*, vol. 10, no. 1. 1995.

[7] K. Dohnalová, T. Gregorkiewicz, and K. Kůsová, "Silicon quantum dots: surface matters.," *J. Phys. Condens. matter*, vol. 26, no. 17, p. 173201, 2014.

[8] J. Heitmann, F. Müller, M. Zacharias, and U. Gösele, "Silicon nanocrystals: Size matters," *Adv. Mater.*, vol. 17, no. 7, pp. 795–803, 2005.

[9] X. Cheng, S. B. Lowe, P. J. Reece, and J. J. Gooding, "Colloidal silicon quantum dots: from preparation to the modification of self-assembled monolayers (SAMs) for bio-applications," *Chem. Soc. Rev.*, vol. 43, p. 2680, 2014.

[10] I. Dogan and M. C. M. van de Sanden, "Direct characterization of nanocrystal size distribution using Raman spectroscopy," *J. Appl. Phys.*, vol. 114, no. 13, p. 134310, 2013.

[11] K. E. Moselund, H. Ghoneim, H. Schmid, M. T. Björk, E. Lörtscher, S. Karg, G. Signorello, D. Webb, M. Tschudy, R. Beyeler, and H. Riel, "Solid-state diffusion as an efficient doping method for silicon nanowires and nanowire field effect transistors.," *Nanotechnology*, vol. 21, no. 43, p. 435202, 2010.

[12] G. Petretto, A. Debernardi, and M. Fanciulli, "Donor wave functions delocalization in silicon nanowires: The peculiar [011] orientation," *Nano Lett.*, vol. 13, no. 10, pp. 4963–4968, 2013.

[13] N. Fukata, J. Kaminaga, R. Takiguchi, R. Rurali, M. Dutta, and K. Murakami, "Interaction of boron and phosphorus impurities in silicon nanowires during low-temperature ozone oxidation," *J. Phys. Chem. C*, vol. 117, pp. 20300–20307, 2013.

[14] R. Guerra and S. Ossicini, "Preferential positioning of dopants and co-dopants in embedded and freestanding Si nanocrystals," *J. Am. Chem. Soc.*, vol. 136, pp. 4404–4409, 2014.

[15] L. Mangolini, "Synthesis, properties, and applications of silicon nanocrystals," *J. Vac. Sci. Technol. B Microelectron. Nanom. Struct.*, vol. 31, no. 2, p. 020801, 2013.

[16] T. Shimizu-Iwayama, N. Kurumado, D. E. Hole, and P. D. Townsend, "Optical properties of silicon nanoclusters fabricated by ion implantation," *J. Appl. Phys.*, vol. 83, no. 11, pp. 6018–6022, 1998.

[17] S. Guha, M. D. Pace, D. N. Dunn, and I. L. Singer, "Visible light emission from Si nanocrystals grown by ion implantation and subsequent annealing," *Appl. Phys. Lett.*, vol. 70, no. 10, pp. 1207–1209, 1997.

[18] G. Ghislotti, B. Nielsen, P. A. Kumar, K. G. Lynn, A. Gambhir, L. F. Di Mauro, and C. E. Bottani, "Effect of different preparation conditions on light emission from silicon implanted SiO2 layers," *Jpn. J. Appl. Phys.*, vol. 79, no. 11, p. 8660, 1996.

[19] W. S. Cheong, N. M. Hwang, and D. Y. Yoon, "Observation of nanometer silicon clusters in the hot-filament CVD process," *J. Cryst. Growth*, vol. 204, no. 1, pp. 52–61, 1999.

[20] L. He, T. Inokuma, Y. Kurata, and S. Hasegawa, "Vibrational properties of SiO and SiH in amorphous SiOx:H films ($0 \leq x \leq 2.0$) prepared by plasma-enhanced chemical vapor deposition," *J. Non. Cryst. Solids*, vol. 185, no. 3, pp. 249–261, 1995.

[21] A. J. Kenyon, P. F. Trwoga, C. W. Pitt, and G. Rehm, "Luminescence efficiency measurements of silicon nanoclusters," *Appl. Phys. Lett.*, vol. 73, no. 4, pp. 523–525, 1998.

[22] M. Perego, M. Fanciulli, C. Bonafos, and N. Cherkashin, "Synthesis of mono and bi-layer of Si nanocrystals embedded in a dielectric matrix by e-beam evaporation of SiO/SiO2 thin films," *Mater. Sci. Eng. C*, vol. 26, no. 5–7, pp. 835–839, 2006.

[23] M. Perego, G. Seguini, C. Wiemer, M. Fanciulli, P.-E. Coulon, and C. Bonafos, "Si nanocrystal synthesis in HfO2/SiO/HfO2 multilayer structures.," *Nanotechnology*, vol. 21, no. 5, p. 055606, 2010.

[24] H. Seifarth, R. Grötzschel, A. Markwitz, W. Matz, P. Nitzsche, and L. Rebohle, "Preparation of SiO2 films with embedded Si nanocrystals by reactive r.f. magnetron sputtering," *Thin Solid Films*, vol. 330, no. 2, pp. 202–205, 1998.

[25] M. Zacharias, H. Freistedt, F. Stolze, T. P. Dr??sedau, M. Rosenbauer, and M. Stutzmann, "Properties of sputtered a-SiOx:H alloys with a visible luminescence," *J. Non. Cryst. Solids*, vol. 164–166, no. 2, pp. 1089–1092, 1993.

[26] S. Furukawa and T. Miyasato, "Quantum size effects on the optical band gap of microcrystalline Si: H," *Phys. Rev. B*, vol. 38, no. 8, pp. 5726–5729, 1988.

[27] J. Valenta, R. Juhasz, and J. Linnros, "Photoluminescence spectroscopy of single silicon quantum dots," *Appl. Phys. Lett.*, vol. 80, no. 6, pp. 1070–1072, 2002.

[28] B. Han, Y. Shimizu, G. Seguini, E. Arduca, C. Castro, G. Ben Assayag, K. Inoue, Y. Nagai, S. Schamm-Chardon, and M. Perego, "Evolution of shape, size, and areal density of a single plane of Si nanocrystals embedded in SiO 2 matrix studied by atom probe tomography," *RSC Adv.*, vol. 6, pp. 3617–3622, 2016.

[29] T. Shimizu-Iwayama, Y. Terao, A. Kamiya, M. Takeda, S. Nakao, and K. Saitoh, "Novel

approach for synthesizing of nanometer-sized Si crystals in SiO2 by ion implantation and their optical characterization," *Nucl. Instruments Methods Phys. Res. Sect. B Beam Interact. with Mater. Atoms*, vol. 112, pp. 214–218, 1996.

[30] P. Dimitrakis, E. Kapetanakis, D. Tsoukalas, D. Skarlatos, C. Bonafos, G. Ben Asssayag, A. Claverie, M. Perego, M. Fanciulli, V. Soncini, R. Sotgiu, A. Agarwal, M. Ameen, C. Sohl, and P. Normand, "Silicon nanocrystal memory devices obtained by ultra-low-energy ion-beam synthesis," *Solid. State. Electron.*, vol. 48, no. 9, pp. 1511–1517, 2004.

[31] N. Cherkashin, C. Bonafos, H. Coffin, M. Carrada, S. Schamm, G. Ben Assayag, D. Chassaing, P. Dimitrakis, P. Normand, M. Perego, M. Fanciulli, T. Muller, K. H. Heinig, and A. Claverie, "Fabrication of nanocrystal memories by ultra low energy ion implantation," *Phys. Status Solidi*, vol. 2, no. 6, pp. 1907–1911, 2005.

[32] A. A. D. T. Adikaari, D. M. N. M. Dissanayake, R. A. Hatton, and S. R. P. Silva, "Efficient laser textured nanocrystalline silicon-polymer bilayer solar cells," *Appl. Phys. Lett.*, vol. 90, no. 20, p. 203514, 2007.

[33] O. M. Nayfeh, S. Rao, A. Smith, J. Therrien, and M. H. Nayfeh, "Thin film silicon nanoparticle UV photodetector," *IEEE Photonics Technol. Lett.*, vol. 16, no. 8, pp. 1927–1929, 2004.

[34] V. Svrcek, I. Pelant, J. Rehspringer, P. Gilliot, D. Ohlmann, and O. Cregut, "Photoluminescence properties of sol – gel derived SiO 2 layers doped with porous silicon," *Mater. Sci. Eng. C*, vol. 19, pp. 233–236, 2002.

[35] M. L. Ostraat, J. W. De Blauwe, M. L. Green, L. D. Bell, H. A. Atwater, and R. C. Flagan, "Ultraclean Two-Stage Aerosol Reactor for Production of Oxide-Passivated Silicon Nanoparticles for Novel Memory Devices," *J. Electrochem. Soc.*, vol. 148, no. 5, pp. G265–G270, 2001.

[36] X. Li, Y. He, S. S. Talukdar, and M. T. Swihart, "Process for preparing macroscopic quantities of brightly photoluminescent silicon nanoparticles with emission spanning the visible spectrum," *Langmuir*, vol. 19, pp. 8490–8496, 2003.

[37] L. Mangolini, E. Thimsen, and U. Kortshagen, "High-Yield Plasma Synthesis of Luminescent Silicon Nanocrystals," *Nano Lett.*, vol. 5, no. 4, pp. 655–659, 2005.

[38] R. M. Sankaran, D. Holunga, R. C. Flagan, and K. P. Giapis, "Synthesis of blue luminescent Si nanoparticles using atmospheric-pressure microdischarges," *Nano Lett.*, vol. 5, no. 3, pp. 537–541, 2005.

[39] T. Nozaki, K. Sasaki, T. Ogino, D. Asahi, and K. Okazaki, "Microplasma synthesis of tunable photoluminescent silicon nanocrystals," *Nanotechnology*, vol. 18, p. 235603, 2007.

[40] M. S. Dresselhaus, G. Chen, M. Y. Tang, R. Yang, H. Lee, D. Wang, Z. Ren, J. P. Fleurial, and P. Gogna, "New directions for low-dimensional thermoelectric materials," *Adv. Mater.*, vol. 19, pp. 1043–1053, 2007.

[41] R. Lechner, H. Wiggers, A. Ebbers, J. Steiger, M. S. Brandt, and M. Stutzmann, "Thermoelectric effect in laser annealed printed nanocrystalline silicon layers," *Phys. Status Solidi - Rapid Res. Lett.*, vol. 1, no. 6, pp. 262–264, 2007.

[42] A. Datta, S. O, F. U. Ying, and M. W. Willander, “Electron Transport in Nanocrystalline Si Based Single Electron Transistors Electron Transport in Nanocrystalline Si Based Single Electron Transistors,” *Jpn. J. Appl. Phys.*, vol. 39, p. 4647, 2000.

[43] K. Nishiguchi and S. Oda, “Electron transport in a single silicon quantum structure using a vertical silicon probe,” *J. Appl. Phys.*, vol. 88, no. 7, p. 4186, 2000.

[44] C.-Y. Liu, Z. C. Holman, and U. R. Kortshagen, “Hybrid Solar Cells from P3HT and Silicon Nanocrystals,” *Nano Lett.*, vol. 9, no. 1, p. 449, 2009.

[45] K. Nishiguchi, X. Zhao, and S. Oda, “Nanocrystalline silicon electron emitter with a high efficiency enhanced by a planarization technique,” *J. Appl. Phys.*, vol. 92, no. 5, pp. 2748–2757, 2002.

[46] D. Jurbergs, E. Rogojina, L. Mangolini, and U. Kortshagen, “Silicon nanocrystals with ensemble quantum yields exceeding 60%,” *Appl. Phys. Lett.*, vol. 88, no. 23, p. 233116, 2006.

[47] K. A. Littau, P. Szajowski, J. Muller, A. Kortan, and L. Brus, “A luminescent Silicon Nanocrystal colloid via a High-Temperature Aereosol Reaction,” *J. Phys. Chem.*, vol. 97, no. 69, p. 1224, 1993.

[48] Q. Xu, J. W. Luo, S. S. Li, J. B. Xia, J. Li, and S. H. Wei, “Chemical trends of defect formation in Si quantum dots: The case of group-III and group-V dopants,” *Phys. Rev. B - Condens. Matter Mater. Phys.*, vol. 75, no. 23, pp. 1–6, 2007.

[49] M. G. Mavros, D. a. Micha, and D. S. Kilin, “Optical Properties of Doped Silicon Quantum Dots with Crystalline and Amorphous Structures,” *J. Phys. Chem. C*, vol. 115, no. 40, pp. 19529–19537, 2011.

[50] A. M. Hartel, D. Hiller, S. Gutsch, P. Löper, S. Estradé, F. Peiró, B. Garrido, and M. Zacharias, “Formation of size-controlled silicon nanocrystals in plasma enhanced chemical vapor deposition grown SiOxNy/SiO2 superlattices,” *Thin Solid Films*, vol. 520, pp. 121–125, 2011.

[51] J. H. Warner, A. Hoshino, K. Yamamoto, and R. D. Tilley, “Water-soluble photoluminescent silicon quantum dots,” *Angew. Chemie - Int. Ed.*, vol. 44, pp. 4550–4554, 2005.

[52] M. Zacharias, J. Heitmann, R. Scholz, U. Kahler, M. Schmidt, and J. Bl??sing, “Size-controlled highly luminescent silicon nanocrystals: A SiO/SiO 2 superlattice approach,” *Appl. Phys. Lett.*, vol. 80, no. 4, pp. 661–663, 2002.

[53] F. Ruffino, L. Romano, E. Carria, M. Miritello, M. G. Grimaldi, V. Privitera, and F. Marabelli, “A combined ion implantation/nanosecond laser irradiation approach towards SI nanostructures doping,” *J. Nanotechnol.*, vol. 2012, 2012.

[54] M. Fujii, S. Hayashi, and K. Yamamoto, “Photoluminescence from B-doped Si nanocrystals,” *J. Appl. Phys.*, vol. 83, no. 1998, pp. 7953–7957, 1998.

[55] H. Gnaser, S. Gutsch, M. Wahl, R. Schiller, M. Kopnarski, D. Hiller, and M. Zacharias, “Phosphorus doping of Si nanocrystals embedded in silicon oxynitride determined by atom probe tomography,” *J. Appl. Phys.*, vol. 115, no. 3, p. 034304, 2014.

[56] M. Perego, G. Seguini, E. Arduca, J. Frascaroli, D. De Salvador, M. Mastromatteo, A. Carnera, G. Nicotra, M. Scuderi, C. Spinella, G. Impellizzeri, C. Lenardi, and E. Napolitani, "Thermodynamic stability of high phosphorus concentration in silicon nanostructures.," *Nanoscale*, vol. 7, no. 34, pp. 14469–75, Aug. 2015.

[57] S. Gutsch, J. Laube, D. Hiller, W. Bock, M. Wahl, M. Kopnarski, H. Gnaser, B. Puthen-Veettil, and M. Zacharias, "Electronic properties of phosphorus doped silicon nanocrystals embedded in SiO2," *Appl. Phys. Lett.*, vol. 106, no. 11, p. 113103, 2015.

[58] D. König, S. Gutsch, H. Gnaser, M. Wahl, M. Kopnarski, J. Göttlicher, R. Steininger, M. Zacharias, and D. Hiller, "Location and Electronic Nature of Phosphorus in the Si Nanocrystal--SiO2 System.," *Sci. Rep.*, vol. 5, p. 09702, 2015.

[59] A. Carvalho, M. J. Rayson, and P. R. Briddon, "Effect of Oxidation on the Doping of Silicon Nanocrystals with Group V Elements," *J. Phys. Chem. C*, vol. 116, p. 8243−8250, 2012.

[60] X. D. Pi, R. Gresback, R. W. Liptak, S. A. Campbell, and U. Kortshagen, "Doping efficiency, dopant location, and oxidation of Si nanocrystals," *Appl. Phys. Lett.*, vol. 92, no. 12, pp. 1–4, 2008.

[61] Y. Ma, X. Chen, X. Pi, and D. Yang, "Lightly boron and phosphorus co-doped silicon nanocrystals," *J. Nanoparticle Res.*, vol. 14, p. 802, 2012.

[62] X. Chen, X. Pi, and D. Yang, "Critical role of dopant location for P-doped Si nanocrystals," *J. Phys. Chem. C*, vol. 115, no. 3, pp. 661–666, 2011.

[63] X. Pi, X. Chen, and D. Yang, "First-principles study of 2.2 nm silicon nanocrystals doped with boron," *J. Phys. Chem. C*, vol. 115, no. 20, pp. 9838–9843, 2011.

[64] X. Pi, "Doping silicon nanocrystals with boron and phosphorus," *J. Nanomater.*, vol. 2012, 2012.

[65] M. Fujii, Y. Yamaguchi, Y. Takase, K. Ninomiya, and S. Hayashi, "Control of photoluminescence properties of Si nanocrystals by simultaneously doping n- and P-type impurities," *Appl. Phys. Lett.*, vol. 85, no. 7, pp. 1158–1160, 2004.

[66] A. Mimura, M. Fujii, S. Hayashi, and K. Yamamoto, "Photoluminescence from Si nanocrystals dispersed in phosphosilicate glass thin films" *J. Lumin.*, vol. 87, no. 1999, pp. 429–431, 2000.

[67] M. Fujii, A. Mimura, S. Hayashi, Y. Yamamoto, and K. Murakami, "Hyperfine Structure of the Electron Spin Resonance of Phosphorus-Doped Si Nanocrystals P concentration P-doped nc-Si" *Phys. Rev. Lett.*, vol. 89, no. 20, p. 206805, 2002.

[68] G. A. Kachurin, S. G. Yanovskaya, D. I. Tetelbaum, and A. N. Mikhailov, "The Effect of implantation of P Ions on the photoluminescence of Si nanocrystals in a SiO_2 layers" *Semiconductors*, vol. 37, no. 6, p. 713, 2003.

[69] Y. Kanzawa, M. Fujii, S. Hayashi, and K. Yamamotob, "Doping of B atoms into Si nanocrystals prepared by RF cosputtering" *Solid State Commun.*, vol. 100, no. 4, pp. 227–230, 1996.

[70] R. Khelifi, D. Mathiot, R. Gupta, D. Muller, M. Roussel, and S. Duguay, "Efficient n-type

doping of Si nanocrystals embedded in SiO 2 by ion beam synthesis," *Appl. Phys. Lett.*, vol. 102, no. 01, p. 013116, 2013.

[71] R. Lechner, A. R. Stegner, R. N. Pereira, R. Dietmueller, M. S. Brandt, A. Ebbers, M. Trocha, H. Wiggers, and M. Stutzmann, "Electronic properties of doped silicon nanocrystal films," *J. Appl. Phys.*, vol. 104, no. 5, p. 053701, 2008.

[72] J. H. Eom, T. L. Chan, and J. R. Chelikowsky, "Vacancies and B doping in Si nanocrystals," *Solid State Commun.*, vol. 150, pp. 130–132, 2010.

[73] G. Cantele, E. Degoli, E. Luppi, R. Magri, D. Ninno, G. Iadonisi, and S. Ossicini, "First-principles study of n- and p-doped silicon nanoclusters," *Phys. Rev. B - Condens. Matter Mater. Phys.*, vol. 72, no. 11, p. 113303, 2005.

[74] A. Carvalho, S. Öberg, M. Barroso, M. J. Rayson, and P. Briddon, "P-doping of Si nanoparticles: The effect of oxidation" *Phys. Status Solidi Appl. Mater. Sci.*, vol. 209, no. 10, pp. 1847–1850, 2012.

[75] F. Iori, E. Degoli, R. Magri, I. Marri, G. Cantele, D. Ninno, F. Trani, O. Pulci, and S. Ossicini, "Engineering silicon nanocrystals: Theoretical study of the effect of codoping with boron and phosphorus" *Phys. Rev. B - Condens. Matter Mater. Phys.*, vol. 76, no. 8, p. 085302, 2007.

[76] J. Ma, S. Wei, N. R. Neale, and A. J. Nozik, "Effect of surface passivation on dopant distribution in Si quantum dots : The case of B and P doping," *Appl. Phys. Lett.*, vol. 98, no. 17, p. 173103, 2011.

[77] A. Carvalho, S. Öberg, M. Barroso, M. J. Rayson, and P. Briddon, "Boron doped Si nanoparticles: the effect of oxidation," *Phys. Status Solidi basic solid state Phys.*, vol. 250, no. 9, pp. 1799–1803, 2013.

[78] A. Carvalho, B. Celikkol, J. Coutinho, and P. R. Briddon, "Surface-phosphorus interaction in Si nanocrystals," *J. Phys. Conf. Ser.*, vol. 281, p. 012027, 2011.

[79] X. D. Pi, R. Gresback, R. W. Liptak, S. A. Campbell, and U. Kortshagen, "Doping efficiency, dopant location, and oxidation of Si nanocrystals," *Appl. Phys. Lett.*, vol. 92, no. 12, pp. 23–25, 2008.

[80] A. R. Stegner, R. N. Pereira, R. Lechner, K. Klein, H. Wiggers, M. Stutzmann, and M. S. Brandt, "Doping efficiency in freestanding silicon nanocrystals from the gas phase: Phosphorus incorporation and defect-induced compensation," *Phys. Rev. B - Condens. Matter Mater. Phys.*, vol. 80, no. 16, pp. 1–10, 2009.

[81] G. Polisski, D. Kovalev, G. Dollinger, T. Sulima, and F. Koch, "Boron in mesoporous Si - where have all the carriers gone?," *Phys. B Condens. Matter*, vol. 273–274, pp. 951–954, 1999.

[82] G. M. Dalpian and J. R. Chelikowsky, "Self-purification in semiconductor nanocrystals," *Phys. Rev. Lett.*, vol. 96, no. 22, p. 226802, 2006.

[83] J. P. Petropoulos, T. R. Cristiani, P. B. Dongmo, and J. M. O. Zide, "A simple thermodynamic model for the doping and alloying of nanoparticles.," *Nanotechnology*, vol. 22, no. 24, p. 245704, 2011.

[84] T. L. Chan, S. B. Zhang, and J. R. Chelikowsky, “An effective one-particle theory for formation energies in doping Si nanostructures,” *Appl. Phys. Lett.*, vol. 98, no. 13, p. 133116, 2011.

[85] T.-L. Chan, A. T. Zayak, G. M. Dalpian, and J. R. Chelikowsky, “Role of Confinement on Diffusion Barriers in Semiconductor Nanocrystals,” *Phys. Rev. Lett.*, vol. 102, no. 2, p. 025901, Jan. 2009.

[86] T. Chan, M. L. Tiago, E. Kaxiras, and J. R. Chelikowsky, “Size Limits on Doping Phosphorus into Silicon Nanocrystals,” *Nano Lett.*, vol. 8, no. 2, pp. 596–600, 2008.

[87] S. C. Erwin, L. Zu, M. I. Haftel, A. L. Efros, T. a Kennedy, and D. J. Norris, “Doping semiconductor nanocrystals,” *Nature*, vol. 436, pp. 91–94, 2005.

[88] S. Ossicini, E. Degoli, F. Iori, E. Luppi, R. Magri, G. Cantele, F. Trani, and D. Ninno, “Simultaneously B- and P-doped silicon nanoclusters: Formation energies and electronic properties,” *Appl. Phys. Lett.*, vol. 87, no. 17, pp. 1–3, 2005.

[89] L. Mangolini and U. Kortshagen, “Plasma-assisted synthesis of silicon nanocrystal inks,” *Adv. Mater.*, vol. 19, pp. 2513–2519, 2007.

[90] R. Gresback, T. Nozaki, and K. Okazaki, “Synthesis and oxidation of luminescent silicon nanocrystals from silicon tetrachloride by very high frequency nonthermal plasma,” *Nanotechnology*, vol. 22, p. 305605, 2011.

[91] Z. Ni, X. Pi, and D. Yang, “Doping Si nanocrystals embedded in SiO<math><msub><mrow></mrow><mn>2</mn></msub></math> with P in the framework of density functional theory,” *Phys. Rev. B*, vol. 89, no. 3, p. 035312, 2014.

[92] N. Garcia-Castello, S. Illera, J. D. Prades, S. Ossicini, A. Cirera, and R. Guerra, “Energetics and carrier transport in doped Si/SiO2 quantum dots,” *Nanoscale*, vol. 7, pp. 12564–71, 2015.

[93] R. N. Pereira and a J. Almeida, “Doped semiconductor nanoparticles synthesized in gas-phase plasmas,” *J. Phys. D. Appl. Phys.*, vol. 48, no. 31, p. 314005, 2015.

[94] Z. Ni, X. Pi, M. Ali, S. Zhou, T. Nozaki, and D. Yang, “Freestanding doped silicon nanocrystals synthesized by plasma,” *J. Phys. D. Appl. Phys.*, vol. 48, no. 31, p. 314006, 2015.

[95] J. Knipping, H. Wiggers, B. Rellinghaus, P. Roth, D. Konjhodzic, and C. Meier, “Synthesis of high purity silicon nanoparticles in a low pressure microwave reactor,” *J. Nanosci. Nanotechnol.*, vol. 4, no. 8, pp. 1039–1044, 2004.

[96] S. Zhou, X. Pi, Z. Ni, Q. Luan, Y. Jiang, C. Jin, T. Nozaki, and D. Yang, “Boron- and phosphorus-hyperdoped silicon nanocrystals,” *Part. Part. Syst. Charact.*, vol. 32, no. 2, pp. 213–221, 2015.

[97] Borowik, T. Nguyen-Tran, P. Roca I Cabarrocas, and T. Mélin, “Doped semiconductor nanocrystal junctions,” *J. Appl. Phys.*, vol. 114, no. 20, p. 204305, 2013.

[98] K. Someno, K. Usami, T. Kodera, Y. Kawano, M. Hatano, and S. Oda, “Photoluminescence of nanocrystalline silicon quantum dots with various sizes and

various phosphorus doping concentrations prepared by very high frequency plasma," *Jpn. J. Appl. Phys.*, vol. 51, no. 11, 2012.

[99] A. Becker, G. Schierning, R. Theissmann, M. Meseth, N. Benson, R. Schmechel, D. Schwesig, N. Petermann, H. Wiggers, and P. Ziolkowski, "A sintered nanoparticle p-n junction observed by a Seebeck microscan," *J. Appl. Phys.*, vol. 111, no. 5, p. 054320, 2012.

[100] S. Zhou, Y. Ding, X. Pi, and T. Nozaki, "Doped silicon nanocrystals from organic dopant precursor by a SiCl4-based high frequency nonthermal plasma," *Appl. Phys. Lett.*, vol. 105, no. 18, pp. 2012–2017, 2014.

[101] A. R. Stegner, R. N. Pereira, K. Klein, R. Lechner, R. Dietmueller, M. S. Brandt, M. Stutzmann, and H. Wiggers, "Electronic transport in phosphorus-doped silicon nanocrystal networks," *Phys. Rev. Lett.*, vol. 100, no. 2, pp. 18–21, 2008.

[102] R. Lechner, A. R. Stegner, R. N. Pereira, R. Dietmueller, M. S. Brandt, A. Ebbers, M. Trocha, H. Wiggers, and M. Stutzmann, "Electronic properties of doped silicon nanocrystal films," *J. Appl. Phys.*, vol. 104, no. 5, 2008.

[103] M. Meseth, K. Lamine, M. Dehnen, S. Kayser, W. Brock, D. Behrenberg, H. Orthner, A. Elsukova, N. Hartmann, H. Wiggers, T. H??lser, H. Nienhaus, N. Benson, and R. Schmechel, "Laser-doping of crystalline silicon substrates using doped silicon nanoparticles," *Thin Solid Films*, vol. 548, pp. 437–442, 2013.

[104] A. R. Stegner, R. N. Pereira, K. Klein, H. Wiggers, M. S. Brandt, and M. Stutzmann, "Phosphorus doping of Si nanocrystals: Interface defects and charge compensation," *Phys. B Condens. Matter*, vol. 401–402, pp. 541–545, 2007.

[105] Y. Nakamine, N. Inaba, T. Kodera, K. Uchida, R. N. Pereira, A. R. Stegner, M. S. Brandt, M. Stutzman, and S. Oda, "Size reduction and phosphorus doping of silicon nanocrystals prepared by a very high frequency plasma deposition system," *Jpn. J. Appl. Phys.*, vol. 50, no. 2, pp. 2–7, 2011.

[106] D. J. Rowe, J. S. Jeong, K. A. Mkhoyan, and U. R. Kortshagen, "Phosphorus-Doped Silicon Nanocrystals Exhibiting Mid-Infrared Localized Surface Plasmon Resonance - Supplementary Information," *Nano Lett.*, p. Supplementary Information, 2013.

[107] H. Kodera, "Constitutional Supercooling during the Crystal Growth of Germanium and Silicon," *Jpn. J. Appl. Phys.*, vol. 2, no. 9, pp. 527–534, 1963.

[108] R. K. Baldwin, J. Zou, K. a Pettigrew, G. J. Yeagle, R. D. Britt, and S. M. Kauzlarich, "The preparation of a phosphorus doped silicon film from phosphorus containing silicon nanoparticles," *Chem. Commun. (Camb).*, no. 6, pp. 658–660, 2006.

[109] K. Fujio, M. Fujii, K. Sumida, S. Hayashi, M. Fujisawa, and H. Ohta, "Electron spin resonance studies of P and B codoped Si nanocrystals," *Appl. Phys. Lett.*, vol. 93, no. 2, p. 021920, 2008.

[110] M. Zacharias, J. Heitmann, R. Scholz, U. Kahler, M. Schmidt, J. Bla, and A. Sio, "M. Zacharias," vol. 80, no. 4, pp. 661–663, 2002.

[111] P. G. Han, Z. Y. Ma, Z. B. Wang, and X. Zhang, "Photoluminescence from intermediate phase silicon structure and nanocrystalline silicon in plasma enhanced chemical vapor

deposition grown Si / SiO 2 multilayers," *Nanotechnology*, vol. 19, p. 325708, 2008.

[112] M. Ishii, I. F. Crowe, M. P. Halsall, A. P. Knights, R. M. Gwilliam, and B. Hamilton, "Luminescence quenching of conductive Si nanocrystals via ' Linkage emission ': Hopping-like propagation of infrared-excited Auger electrons," *J. Appl. Phys.*, vol. 116, no. 06, p. 063513, 2014.

[113] I. Sychugov, J. Valenta, K. Mitsuishi, and J. Linnros, "Exciton localization in doped Si nanocrystals from single dot spectroscopy studies," vol. 075311, pp. 1–6, 2012.

[114] M. Fujii, S. Hayashi, K. Yamamoto, M. Fujii, S. Hayashi, and K. Yamamoto, "Photoluminescence from B-doped Si nanocrystals," *J. Appl. Phys.*, vol. 83, no. 12, p. 7953, 1998.

[115] M. Xie, D. Li, L. Chen, F. Wang, X. Zhu, D. Yang, M. Xie, D. Li, L. Chen, F. Wang, X. Zhu, and D. Yang, "The location and doping effect of boron in Si nanocrystals embedded silicon oxide film The location and doping effect of boron in Si nanocrystals embedded silicon oxide film," vol. 123108, no. 2013, 2016.

[116] M. Fujii, A. Mimura, S. Hayashi, and K. Yamamoto, "Photoluminescence from Si nanocrystals dispersed in phosphosilicate glass thin films : Improvement of photoluminescence efficiency," *Appl. Phys. Lett.*, vol. 75, no. 2, p. 184, 1999.

[117] A. Mimura, D. Kovalev, and F. Koch, "Photoluminescence and free-electron absorption in heavily phosphorus-doped Si nanocrystals," vol. 62, no. 19, pp. 625–627, 2000.

[118] M. Fujii, Y. Yamaguchi, Y. Takase, K. Ninomiya, and S. Hayashi, "Control of photoluminescence properties of Si nanocrystals by simultaneously doping n- and p-type impurities," *Appl. Phys. Lett.*, vol. 85, no. 7, p. 1158, 2004.

[119] S. Gutsch, a. M. Hartel, D. Hiller, N. Zakharov, P. Werner, and M. Zacharias, "Doping efficiency of phosphorus doped silicon nanocrystals embedded in a SiO2 matrix," *Appl. Phys. Lett.*, vol. 100, no. 23, p. 233115, 2012.

[120] M. Zacharias, J. Heitmann, R. Scholz, U. Kahler, M. Schmidt, J. Bläsing, M. Zacharias, J. Heitmann, R. Scholz, and U. Kahler, "Size-controlled highly luminescent silicon nanocrystals : A SiO/SiO_2 superlattice approach," vol. 661, no. 2002, pp. 2–5, 2015.

[121] M. Perego, C. Bonafos, and M. Fanciulli, "Phosphorus doping of ultra-small silicon nanocrystals" *Nanotechnology*, vol. 21, no. 2, p. 025602, 2010.

[122] M. Perego, G. Seguini, and M. Fanciulli, "ToF-SIMS study of phosphorus diffusion in low-dimensional silicon structures" *Surf. Interface Anal.*, vol. 45, no. 1, pp. 386–389, 2013.

[123] C. Eun-Chel, P. Sangwook, H. Xiaojing, S. Dengyuan, C. Gavin, P. Sang-Cheol, and A. G. Martin, "Silicon quantum dot/crystalline silicon solar cells," *Nanotechnology*, vol. 19, no. 24, p. 245201, 2008.

[124] A. I. Kovalev, D. L. Wainstein, D. I. Tetelbaum, W. Hornig, and Y. N. Kucherehko, "Investigation of the electronic structure of the phosphorus-doped Si and SiO_2: Si quantum dots by XPS and HREELS methods" *Surf. Interface Anal.*, vol. 36, pp. 959–962, 2004.

[125] K. Murakami, R. Shirakawa, M. Tsujimura, N. Uchida, N. Fukata, and S. I. Hishita, "Phosphorus ion implantation in silicon nanocrystals embedded in SiO2," *J. Appl. Phys.*, vol. 105, no. 5, pp. 1–6, 2009.

[126] A. L. Tchebotareva, M. J. A. De Dood, J. S. Biteen, H. A. Atwater, and A. Polman, "Quenching of Si nanocrystal photoluminescence by doping with gold or phosphorous," *J. Lumin.*, vol. 114, no. 2, pp. 137–144, 2005.

[127] M. Perego, G. Seguini, E. Arduca, J. Frascaroli, D. De Salvador, M. Mastromatteo, A. Carnera, G. Nicotra, M. Scuderi, C. Spinella, G. Impellizzeri, C. Lenardi, and E. Napolitani, "Thermodynamic stability of high phosphorus concentration in silicon nanostructures," *Nanoscale*, vol. 7, no. 34, pp. 14469–14475, 2015.

[128] M. Mastromatteo, E. Arduca, E. Napolitani, G. Nicotra, D. De Salvador, L. Bacci, J. Frascaroli, G. Seguini, M. Scuderi, G. Impellizzeri, C. Spinella, M. Perego, and A. Carnera, "Quantification of phosphorus diffusion and incorporation in silicon nanocrystals embedded in silicon oxide," *Surf. Interface Anal.*, Nov. 2014.

[129] M. Mastromatteo, E. Arduca, E. Napolitani, G. Nicotra, D. De Salvador, L. Bacci, J. Frascaroli, G. Seguini, M. Scuderi, G. Impellizzeri, C. Spinella, M. Perego, and A. Carnera, "Modeling of phosphorus diffusion in silicon oxide and incorporation in silicon nanocrystals," *J. Mater. Chem. C*, vol. 4, p. 3531, 2016.

[130] U. Fano, "Effects of configuration interaction on intensities and phase shifts," *Phys. Rev.*, vol. 124, no. 6, pp. 1866–1878, 1961.

[131] S. Zhou, X. Pi, Z. Ni, Y. Ding, Y. Jiang, C. Jin, and C. Delerue, "Comparative Study on the Localized Surface Plasmon Resonance Silicon Nanocrystals," *ACS Nano*, no. 1, pp. 378–386, 2015.

[132] A. J. Almeida, H. Sugimoto, M. Fujii, M. S. Brandt, M. Stutzmann, and R. N. Pereira, "Doping efficiency and confinement of donors in embedded and free standing Si nanocrystals," *Phys. Rev. B - Condens. Matter Mater. Phys.*, vol. 93, no. 11, p. 115425, 2016.

[133] R. N. Pereira, S. Niesar, W. B. You, A. F. Da Cunha, N. Erhard, A. R. Stegner, H. Wiggers, M. G. Willinger, M. Stutzmann, and M. S. Brandt, "Solution-processed networks of silicon nanocrystals: The role of internanocrystal medium on semiconducting behavior," *J. Phys. Chem. C*, vol. 115, no. 41, pp. 20120–20127, 2011.

[134] M. Perego, C. Bonafos, and M. Fanciulli, "Phosphorus doping of ultra-small silicon nanocrystals," vol. 025602.

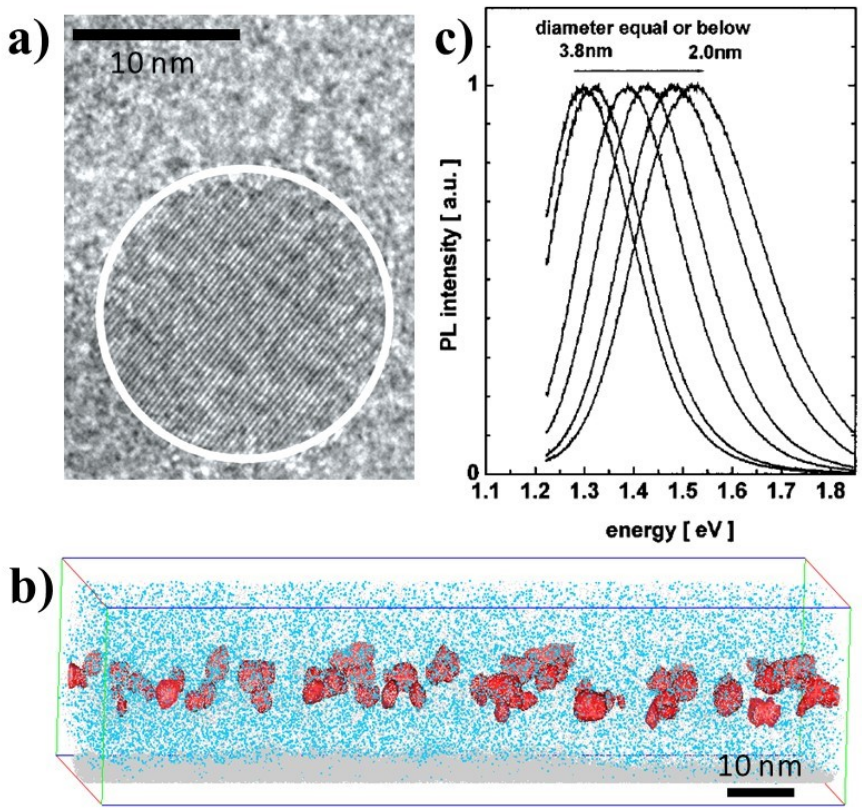

Figure 1 – a) HRTEM of a small Si-NC with spherical and mono-crystalline morphology, reprinted from Dogan *et al.* [10] b) 3D atom map of a Si NCs layer embedded in a SiO_2 matrix obtained by APT [28] c) Normalized photoluminescence spectra showing a blue shift correlated with the crystal size, reprinted from Zacharias *et al.* [52]

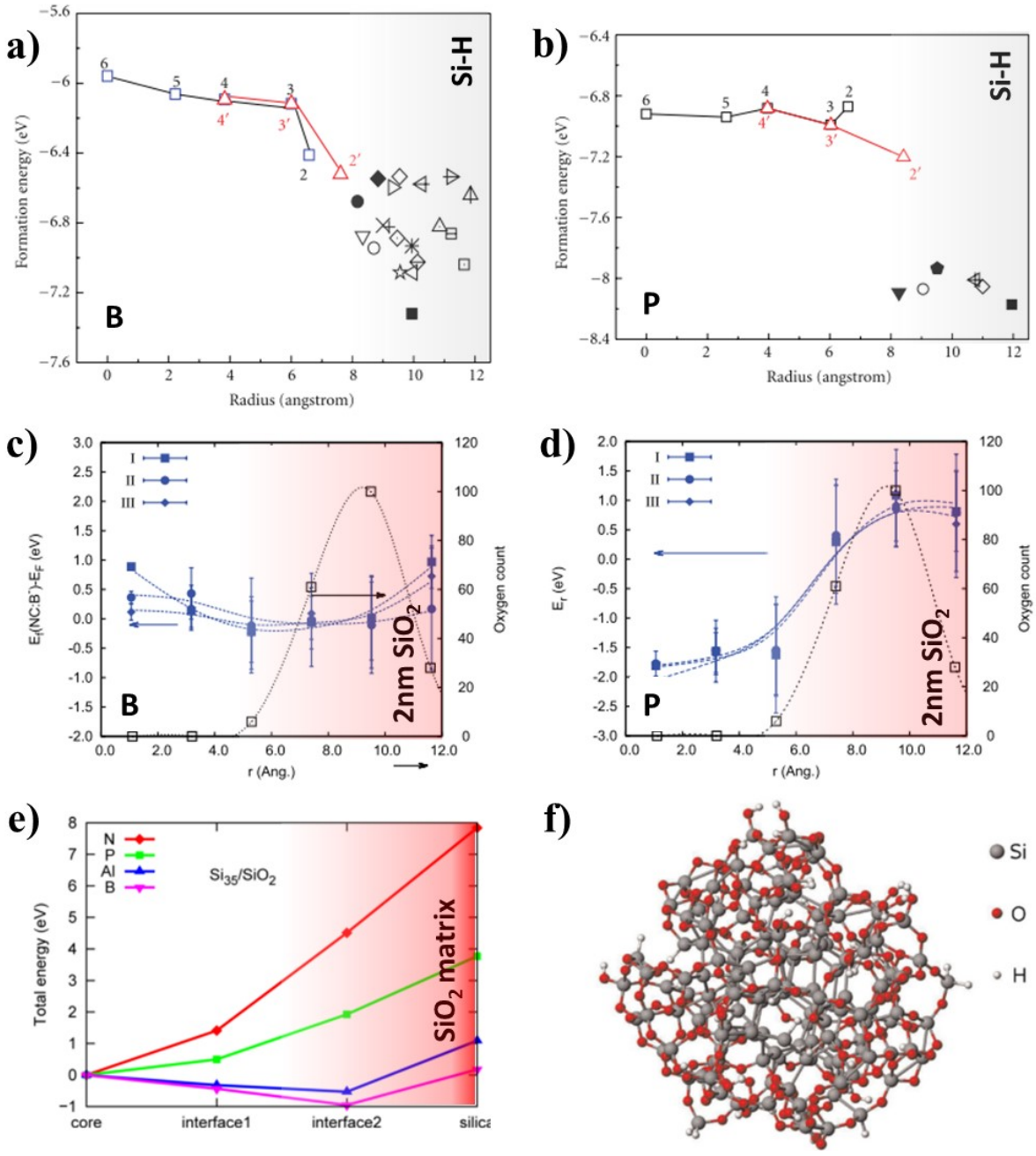

Figure 2 – a) Formation energy of B impurities in H terminated Si NCs for a variety of configuration as a function of the distance from the Si NCs core. Internal substitutional B atoms from subsurface to the NC center (2(2')→3(3')→4(4')→5→6) are shown. Picture adapted from [31]; b) same as previously for P. Picture adapted from and Cheng at al [33]; c) Relative energy of the 2 nm SiO_2-covered Si NCs doped with B as a function of the distance from the centre. Three models for the structure of the nanocrystal were constructed as results of molecular dynamics simulations of 1800 Kanneals during 2.0 ps (I), 2.3 ps (II), and 2.6 ps (III). Open squares represent the distribution of oxygen (coincident for I, II,and III). Picture adapted from Carvalho *et al.* [50]; d) same as previously for P. Picture adapted from Carvalho *et al.* [50]; e) Total energy of the 35 Si atom NC embedded in the SiO_2 structure and doped with N, P, Al, or B atoms. The impurities are introduced as substitutional of a Si atom in the NC center (core), at the interface bonded to one or two oxygens (interface1, interface2), or in the SiO_2 far from the NC (silica). For a better comprehensibility each line has been shifted so that the structure with the dopant in the NC center has zero energy. Picture adapted from Guerra *et al.* [14]; f) example of structure of the undoped 2 nm SiO_2-covered nanoparticle, obtained from molecular dynamics simulations, as printed in [49].

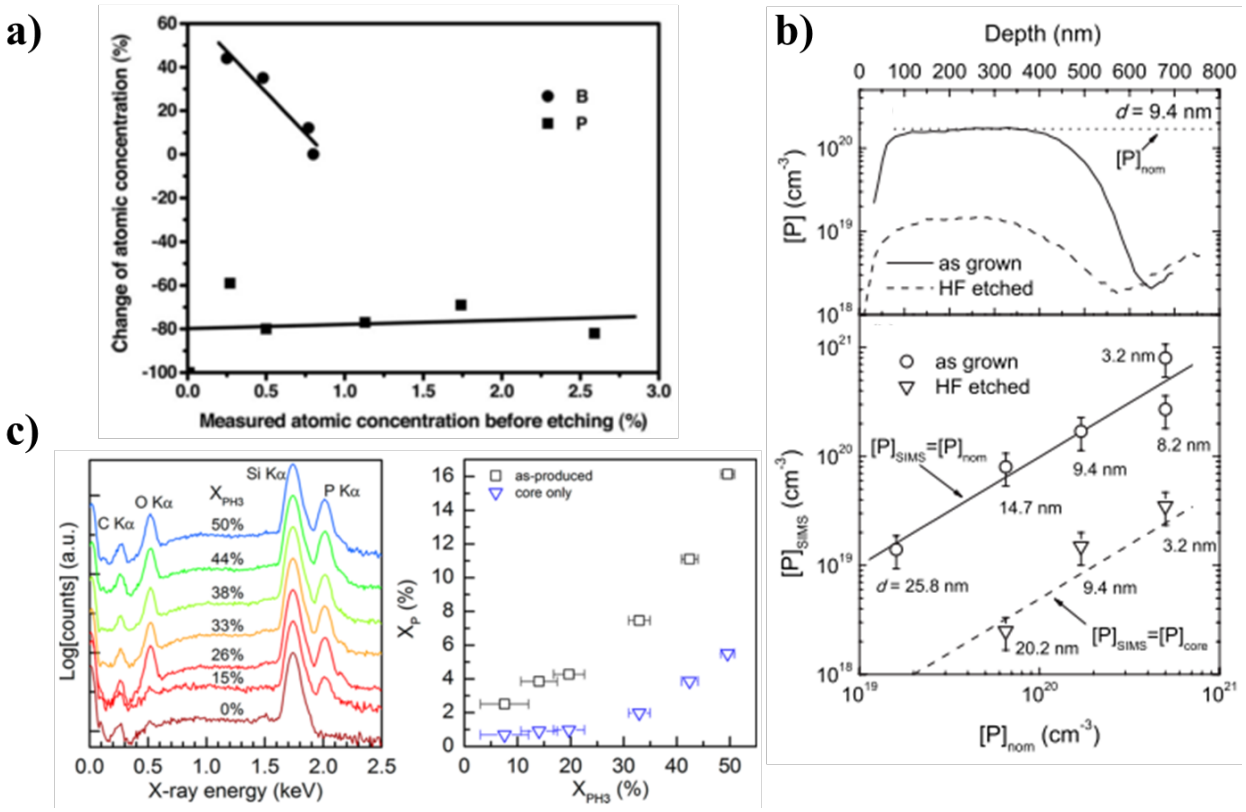

Figure 3 – a) change of dopant concentration after HF etching of 3.6 nm size Si NCs synthetized by nonthermal plasma, as printed by Pi *et al.* [60]; b) top: SIMS profiles of thin films of Si-NCs with a mean diameter of 9.4 nm syntehtized by low pressure mcirowave plasma. $[P]_{nom}$, calculated as the fraction of phosphine in the total flow of precursor gases (SiH_4 and PH_3) multiplied by the atomic density of Si, corresponds to $[P]_{nom}=1.7\ 10^{20}\ cm^{-3}$, the solid curve shows the profile of the as-deposited film, the dashed curve was measured after HF etching. Bottom: Measured P concentration, $[P]_{SIMS}$, extracted from the plateau regions of the SIMS profiles, versus $[P]_{nom}$ before (circles) and after etching in HF (triangles). The data points are labeled with the mean Si NC diameter of the measured samples. The solid line correspond to $[P]_{SIMS}=[P]_{nom}$ and the dashed line shows $[P]_{SIMS}=[P]_{nom}/ 20$. Figure reprinted from Stegner *et al.* [80] ; c) Left: Semilog plot of SEM-EDX spectra of as-produced Si NCs synthetized by RF capacitively coupled nonthermal plasma for varying fractional PH_3 flow rate (X_{PH3}). C, O, Si, and P Kα lines are identified at 0.277, 0.525, 1.74, and 2.01 keV respectively. Oxygen and carbon contaminations are estimated at less than 3 at% and are the result of air exposure during sample transfer. Spectra are offset vertically for clarity. Right: estimated atomic P concentration X_P from SEM-EDX spectra for as produced samples (squares) and for samples after surface P had been removed to probe the Si NC core (inverted triangles). Picture reproduced from Rowe *et al.* [106]

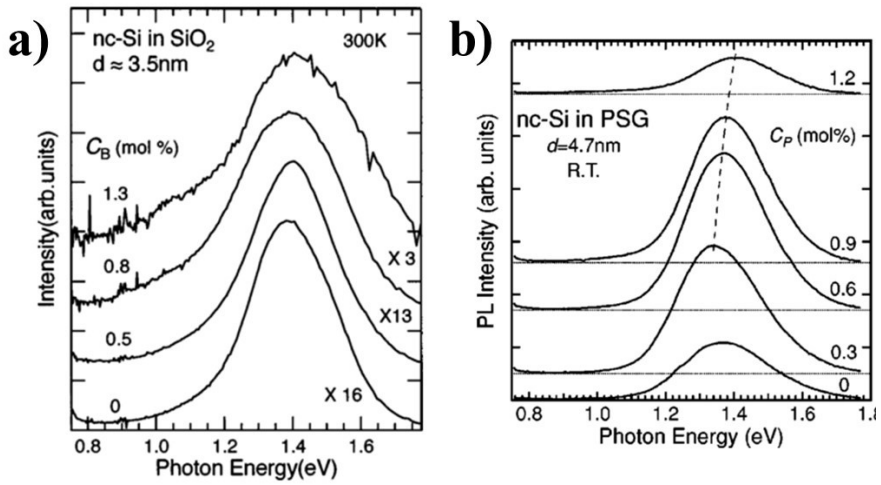

Figure 4 – a) PL spectra of B doped 3.5 nm size Si NCs synthetized by cosputteruing method. C_B is the concentration (mol %) of B_2O_3 in the matrix region estimated from IR absorption spectra. Picture reproduced from Fujii *et al.* [114]; b) Photoluminescence from P doped 4.7 nm size Si NCs dispersed in PSG thin films. The average concentration of P_2O_5 in the films C_P (mol%) was determined by electron probe microanalysis. Picture as printed in Mimura *et al.* [117]

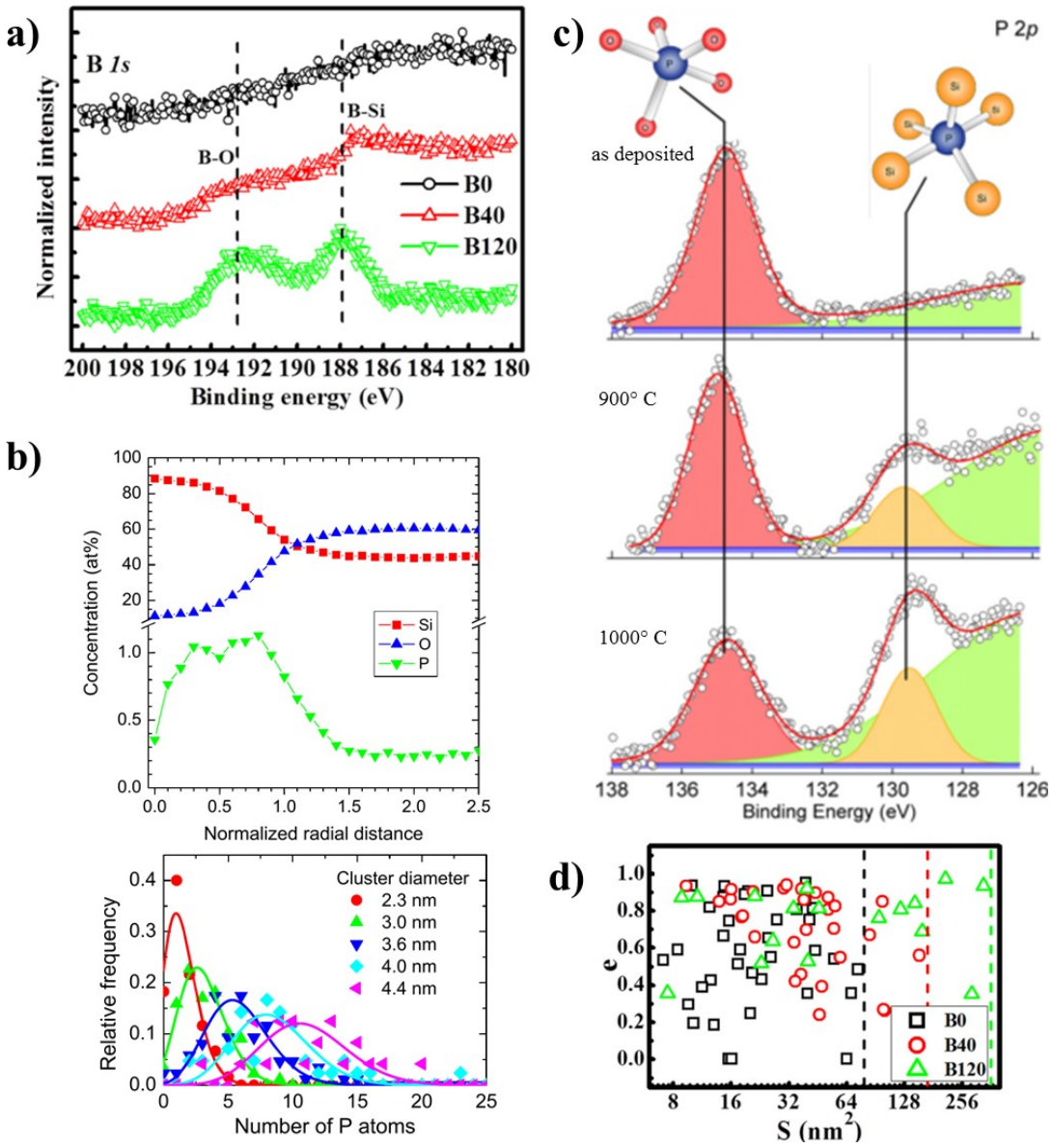

Figure 5 – a) XPS high resolution spectra of B 1*s* core level region for different B concentrations: 0 at.% (B0), 0.59 at.% (B40) and 5.43 at.% (B120). Si NCs were synthetized by cosputtering method and their diameter ranges from 2 to 15 nm. B concentration is estimated by quantified XPS analysis. Figure as printed in Xie *et al.* [115]; b) Top: APT cluster concentration radial profile for the elements Si, O, and P for Si NCs arranged in a superlattices. The extension of all clusters is normalized to a distance between 0 and 1. Data with abscissa-values of <1.0 would correspond to the interior of the Si NCs. Bottom: Poisson distribution fits (solid lines) for the number of P atoms within Si NCs of different size derived from the APT cluster analysis. Figures adapted from Gnaser *et al*. [55]; c) High resolution XPS spectra of the P 2*p* region for the as-deposited, 900 ◦C and 1000 ◦C annealed samples. Si NCs with average diameter equal or smaller than 2nm are arranged in a superlattices. Figure reproduced from Perego *et al.* [134]; d) Statistical analysis on the shape (eccentricity, *e*) and size (cross-sectional area, S) of Si-NCs from HRTEM images for different B concentration: 0 at.% (B0), 0.59 at.% (B40) and 5.43 at.% (B120).. Figure reproduced from Xie *et al.* [115]

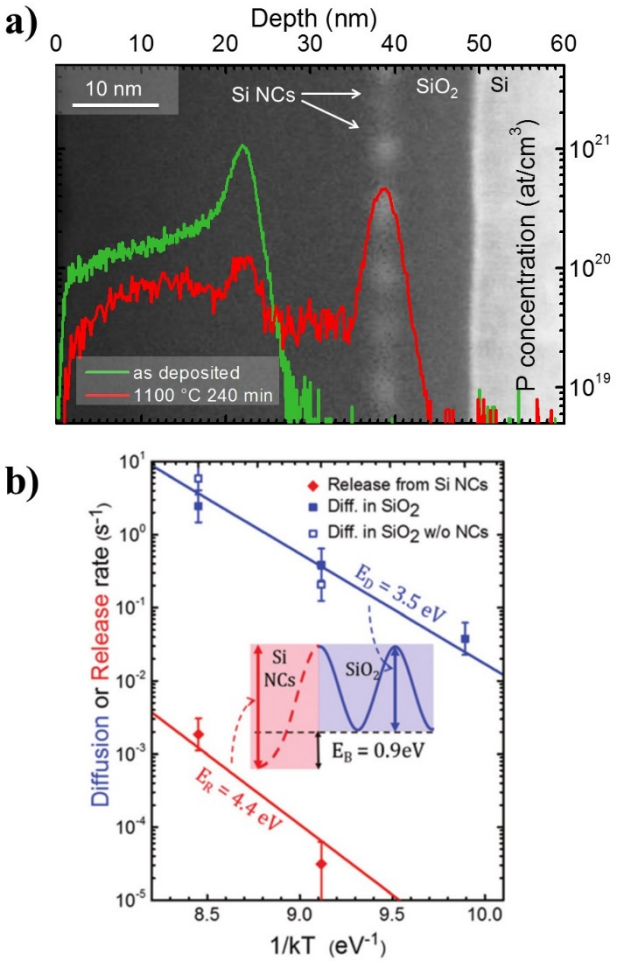

Figure 6 – Layer of 4 nm Si NCs embedded in a SiO_2 matrix prepared by e-beam evaporation and susequent annelaing at hgih temperature. a) ToF-SIMS profiles of the as deposited (green) and annealed (1100 °C, 4 hours, red) samples overlapped with the EFTEM cross sectional image of the as deposited sample; (b) P diffusion (release) rates from Si NCs are reported with filled blue squares (red). Data relative to reference SiO_2 samples are reported (blue empty). The Arrhenius fit of experimental diffusion (release) rates is reported (solid line). The inset depicts the entire energy scheme. Figures adapted from Perego *et al*. [56].

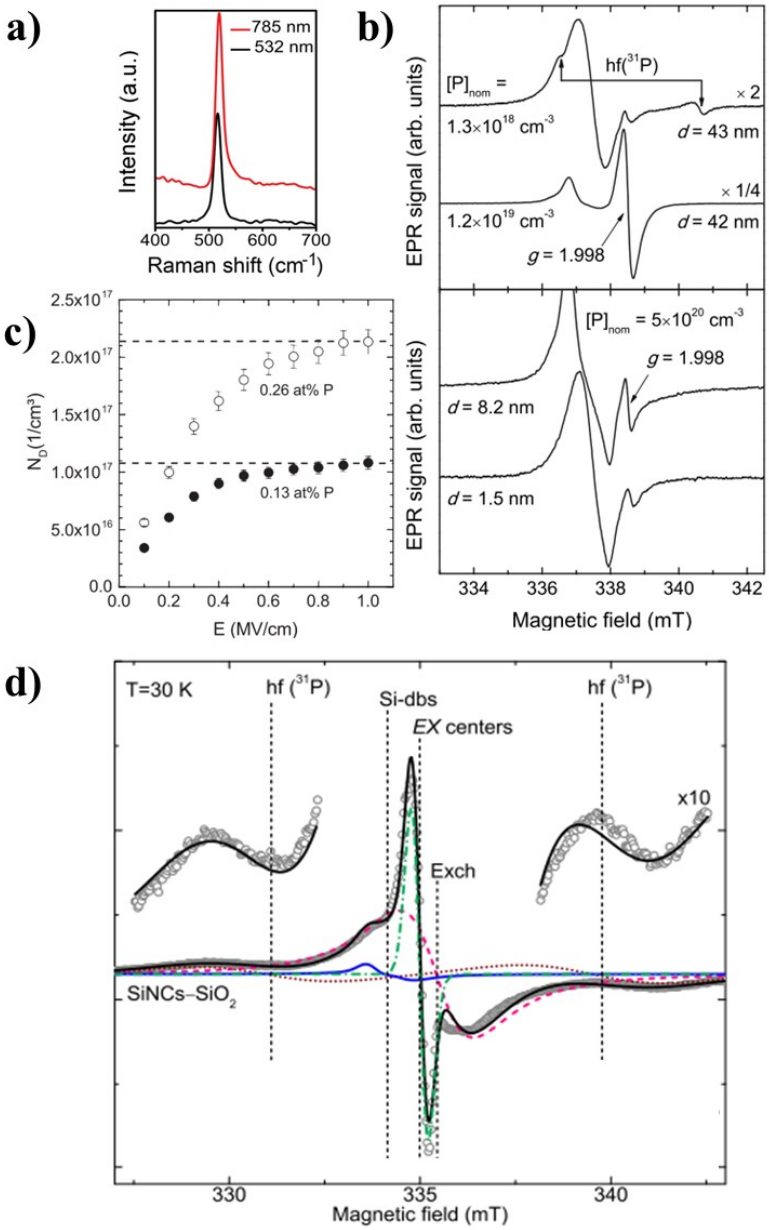

Figure 7 – a) Raman spectra of ≈14 nm Si NCs hyperdoped with B at the concentration of 7% by means of thermal plasma. Data were obtained with lasers operating at the excitation wavelengths of 532 and 785 nm. Picture reproduced from Zhou *et al.* [96]; b) Top: EPR spectra of Si NCs with a mean diameter of 42 and 43 nm grown in a low-pressure microwave plasma reactor, with different P nominal concentration. Bottom: EPR spectra of doped Si-NCs with mean diameters of 8.2 and 1.5 nm grown in a low-pressure microwave plasma reactor at constant P nominal concentration. Pictures as printed in Stegner *et al.* [80]; c) free carrier density calculation from transient current analysis for sample with different total P concentration involved in the synthesis process is plotted as a function of bias voltage. 4 nm size Si NCs are arranged in superlattices and synthetized by PECVD method. Figure as printed in Gutsch *et al*. [57]; d) EPR spectra of 5 nm size Si NCs embedded in SiO_2 matrix synthetized by cosputtering method and its numerical fit. Picture as printed in Almeida *et al.* [132]